

$\pi\pi$ Scattering up to 1.4 GeV of Dipion Mass*B. Y. OH,† A. F. GARFINKEL,‡ R. MORSE, AND W. D. WALKER
Physics Department, University of Wisconsin, Madison, Wisconsin 53706

AND

J. D. PRENTICE, E. C. WEST, AND T. S. YOON
Physics Department, University of Toronto, Toronto, Ontario, Canada

(Received 2 January 1970)

$\pi\pi$ scattering up to 1.4 GeV of dipion mass is studied from the reactions $\pi^-p \rightarrow \pi^- \pi^+ n$ and $\pi^- \pi^0 p$ at 7 GeV/c, using the formalism of absorption-modified one-pion exchange (OPE) with dipion in S , P , and D waves. We limit our analysis to small momentum transfers to the nucleon, including the nucleon-pole terms as background. The ρ^0 , ρ^- , and f^0 mesons, and the $\pi^- \pi^+$ anomaly in the 1.0–1.2-GeV region are analyzed. The S -, P -, and D -wave $\pi\pi$ phase shifts and inelasticities, of isospin 0, 1, and 2, are obtained.

I. INTRODUCTION

THE $\pi\pi$ phase shifts up to a dipion mass of 1 GeV have been carried out by many authors,^{1,2} based on the low-energy data (laboratory momentum $\lesssim 4$ GeV/c) of the reactions $\pi^- p \rightarrow \pi^- \pi^+ n$, $\pi^- p \rightarrow \pi^- \pi^0 p$, and somewhat meager data of the reactions $\pi^- p \rightarrow \pi^0 \pi^0 n$ and $\pi^+ n \rightarrow \pi^0 \pi^0 p$.³ In extracting $\pi\pi$ phase shifts from the reactions $\pi N \rightarrow \pi \pi N$, one attempts an extrapolation in the variable t , squared four momentum transfer to the nucleon, from the physical region to the unphysical mass-shell point. Various authors differ in their methods of this extrapolation; for example, some include the absorption effect, off-shell correction factor, or such questions as the relative phase difference between partial waves in the in and out states of the $\pi\pi$ vertex.^{4–8}

The results of $I=0$ S -wave phase shifts are still

controversial,^{1,2} but in general they fall into two categories: (i) a smooth variation of δ_S^0 in the ρ region, probably reaching 90° at ~ 1 GeV; (ii) alternatively, δ_S^0 varying rapidly and passing through 90° near 0.7–0.8 GeV (a narrow resonance). The $I=2$ S -wave phase shift is small and negative,² reaching about -20° at ~ 1 GeV. An $I=1$ P -wave resonance is given by the ρ meson itself. When the dipion mass is greater than 1 GeV, D -wave scattering can no longer be neglected. Starting at around 1.0–1.1 GeV, the inelastic channels seem to open up, particularly in the $I=0$ S wave and $I=1$ P wave. Our results on the f meson show that the $I=0$ D wave also becomes inelastic in the f region (the study of the f -meson decay into channels other than $\pi^- \pi^+$ is still only preliminary,^{9,10} but indications are that η_D^0 is appreciably less than 1 in the central region of the f). The $\pi\pi$ scattering at still higher energy (≥ 1.6 GeV) is almost diffractive, as evidenced by the prominent forward peak in the $\cos\theta$ distributions.

Below 1.4 GeV in dipion mass, we show that the S -, P -, and D -wave scatterings can explain the data quite well. $l \geq 3$ waves can be neglected to a good approximation, judging from the $\cos\theta$ distributions and the g -meson ($J^P=3^-$) resonance shape, which indicates very small δ_P^1 below 1.5 GeV in dipion mass. We use the absorption-modified one-pion-exchange (AOPE) model^{11,12} in extracting $\pi\pi$ phase shifts up to 1.4 GeV in dipion mass from the reactions

$$\pi^- p \rightarrow \pi^- \pi^+ n \quad (4191 \text{ events}, 1.35 \pm 0.11 \text{ mb}), \quad (1)$$

$$\pi^- p \rightarrow \pi^- \pi^0 p \quad (3555 \text{ events}, 0.85 \pm 0.10 \text{ mb}) \quad (2)$$

at 7 GeV, as obtained from an exposure of 370 000 pictures in the 30-in. MURA-Argonne chamber at the ZGS. The fitting program DIANA was used at Wisconsin, and HGEOM-GRIND at Toronto. Events were selected

* Supported in part by the U.S. Atomic Energy Commission under Contract No. AT(11-1)-881, COO-881-211, and by the National Research Council of Canada.

† Now at Michigan State University, East Lansing, Mich.

‡ Now at Purdue University, Lafayette, Ind.

¹ V. Hagopian, W. Selove, J. Alliti, J. P. Baton, M. Neveu-Rene, R. Gessalori, and A. Romano, Phys. Rev. Letters **14**, 1077 (1965); L. W. Jones, P. O. Caldwell, B. Zacharov, D. Harting, E. Bleuler, W. C. Middlekoop, and B. Elsners, Phys. Letters **21**, 591 (1966); L. J. Gutay, P. B. Johnson, F. S. Loeffler, R. L. McIlwain, D. H. Miller, R. B. Willmann, and P. L. Csonka, Phys. Rev. Letters **18**, 142 (1967).

² W. D. Walker, J. Carroll, A. Garfinkel, and B. Y. Oh, Phys. Rev. Letters **18**, 630 (1967); J. P. Baton, G. Laurens, and J. Reignier, Phys. Letters **25B**, 419 (1967); E. Malamud and P. Schlein, Phys. Rev. Letters **19**, 1056 (1967); S. Marateck *et al.*, *ibid.* **21**, 1613 (1968).

³ J. F. Corbett, C. J. S. Damerell, N. Middlemas, D. Newton, A. B. Clegg, W. S. C. Williams, and A. S. Carroll, Phys. Rev. **156**, 1451 (1967); K. J. Braun, D. Cline, and V. Scherer, Phys. Rev. Letters **21**, 1275 (1968); G. A. Smith and R. J. Manning, *ibid.* **23**, 335 (1969).

⁴ Other methods of getting at the $\pi\pi$ phase shifts are based on backward πN scattering (Ref. 5) or from $K \rightarrow 2\pi$ decay (Ref. 6) at the K -meson mass, or from the reaction (Ref. 7) $\bar{p}p \rightarrow 3\pi$. Still further information, applicable to low dipion mass, comes from a study (Ref. 8) of the decay $K^+ \rightarrow e^+ \nu \pi^+ \pi^-$.

⁵ C. Lovelace, R. M. Heinz, and A. Donnachie, Phys. Letters **22**, 332 (1966).

⁶ S. Bennett, N. Nygren, H. Saal, J. Steinberger, and J. Sunderland, Phys. Rev. Letters **19**, 993 (1967).

⁷ J. F. L. Hopkinson and R. G. Roberts, CERN Report No. TH.911, 1968 (unpublished).

⁸ A. Pais and S. Treiman, Phys. Rev. **168**, 1888 (1968), and references therein.

⁹ W. Beusch, W. E. Fischer, B. Gobbi, M. Peppin, E. Polgar, P. Astbury, G. Brautti, G. Finocchiaro, J. C. Lassale, A. Michelini, K. M. Terwilliger, D. Websdale, and C. H. West, Phys. Letters **25B**, 357 (1967).

¹⁰ G. Ascoli, H. B. Crawley, D. W. Mortara, and A. Shapiro, Phys. Rev. Letters **21**, 1712 (1968).

¹¹ K. Gottfried and J. D. Jackson, Nuovo Cimento **34**, 735 (1964).

¹² L. Durand III and Y. T. Chiu, Phys. Rev. **139**, B646 (1965).

with long secondary pion tracks (>25 cm) and with no secondary interactions, thus obtaining a mass resolution of about 15 and 20 MeV in the 1.0–1.4-GeV region of dipion mass for the reactions (1) and (2), respectively. The dipion mass spectra for these reactions are shown in Fig. 1. Also shown in Fig. 1 for comparison are the four-pion masses for the reactions $\pi^-p \rightarrow \pi^- \pi^+ \pi^- \pi^+ n$ and $\pi^-p \rightarrow \pi^- \pi^+ \pi^- \pi^0 p$ from the same film.¹³

In Sec. II we give an outline of the method of analysis and the result of our method when applied to the ρ meson. It is seen that AOPE can adequately describe the production and decay of the ρ^0 , for $-t < 0.3$ (GeV/c)², while ω exchange contributes significantly to the ρ^- case. The f -meson region and 1.0–1.2-GeV region are analyzed next in Sec. III. The f shows considerable inelasticity. A peculiar behavior of the $\pi^- \pi^+$ state in the 1.0–1.2-GeV region is shown to be either an $I=0$ resonant D -wave amplitude which interferes with a nearly static $I=1$ P -wave amplitude or a moving P -wave (possibly resonant) amplitude which interferes with a rising D wave (f meson). The phase shifts and inelasticities of the S , P , and D waves up to 1.4 GeV in dipion mass are given at the end of Sec. III. Finally we give some discussions in Sec. IV. In Appendices A and B are given the summary of the AOPE amplitudes. Nucleon-pole terms¹⁴ are given in Appendix C.

II. OUTLINE OF METHOD AND ρ MESON

The AOPE model is known to be quite reliable in describing detailed production and decay correlations of the reaction $\pi^-p \rightarrow \rho N$.^{11,12} Thus with a proper account of the background, we could probably explain the data of the reactions (1) and (2) in the region $m_{\pi\pi} < 1$ GeV, where S - and P -wave $\pi\pi$ interactions are expected to dominate ($\eta=1$ for complete elasticity). For the case of the D -wave dipion ($\pi^-p \rightarrow f n$),¹⁵ application of AOPE is somewhat uncertain. The difficulties here are largely owing to (i) an unknown background, (ii) uncertainty in η ($I=0, l=2$) and phase shifts of other waves present, (iii) the problem of off-mass-shell correction, which is already encountered for P -wave values, becoming magnified with higher l values. We assume in this paper the validity of the AOPE for the S -, P -, and D -wave $\pi\pi$ scattering with an off-mass-shell correction in the $\pi\pi$ vertex in a form suggested by Dürr and Pilkuhn¹⁶ (see below).

¹³ Cross sections for these reactions are 1.21 ± 0.11 and 1.61 ± 0.12 mb, respectively. The various cross sections have been determined from measurements on a subsample of the total exposure. For the analysis of g meson from these reactions, as well as reactions (1) and (2), see T. F. Johnston, J. D. Prentice, N. R. Steenberg, T. S. Yoon, A. F. Garfinkel, R. Morse, B. Y. Oh, and W. D. Walker, Phys. Rev. Letters **20**, 1414 (1968).

¹⁴ E. West, J. Boyd, A. Erwin, and W. D. Walker, Phys. Rev. **149**, 1089 (1966).

¹⁵ For earlier absorption-model calculation of the f , see H. Hogaasen, J. Hogaasen, R. Keyser, and B. E. Y. Svenson, Nuovo Cimento **42A**, 323 (1966); P. C. M. York and D. Gordon, Phys. Rev. **157**, 1362 (1967).

¹⁶ H. P. Dürr and H. Pilkuhn, Nuovo Cimento **40**, 899 (1965).

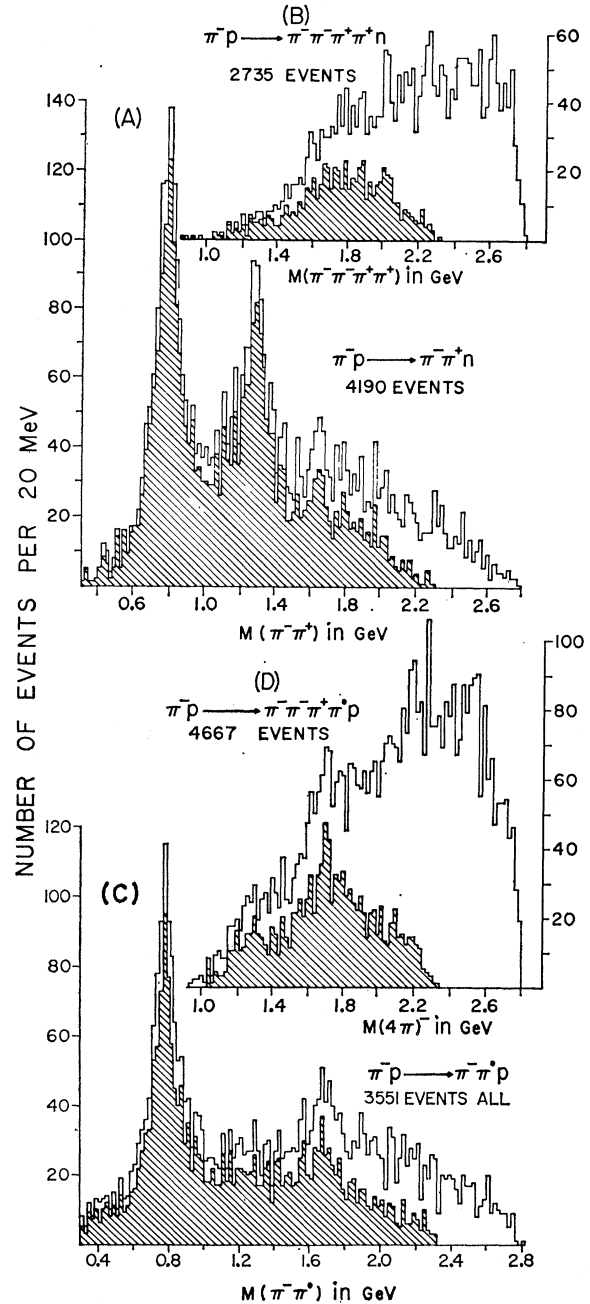


FIG. 1. 2π and 4π mass spectra from the reactions (a) $\pi^-p \rightarrow \pi^- \pi^+ n$, (b) $\pi^-p \rightarrow \pi^- \pi^+ \pi^- \pi^+ n$, (c) $\pi^-p \rightarrow \pi^- \pi^+ \pi^- \pi^+ p$, and (d) $\pi^-p \rightarrow \pi^- \pi^+ \pi^- \pi^+ p$. The events with $-t(=\Delta^2) < 0.3$ (GeV/c)² are shaded.

We use the AOPE formalism of Durand and Chiu¹² in this paper, limiting our analysis to the region of t ($-t < 0.3$ GeV^2/c^2) where it should be reliable. We also include in our amplitudes the effect of the nucleon-pole terms,¹⁴ which we take as the most important background for the t region under consideration [the reflection of N^* 's (1.24, 1.47, 1.68, etc.) production contributes very little compared to the pion-exchange process

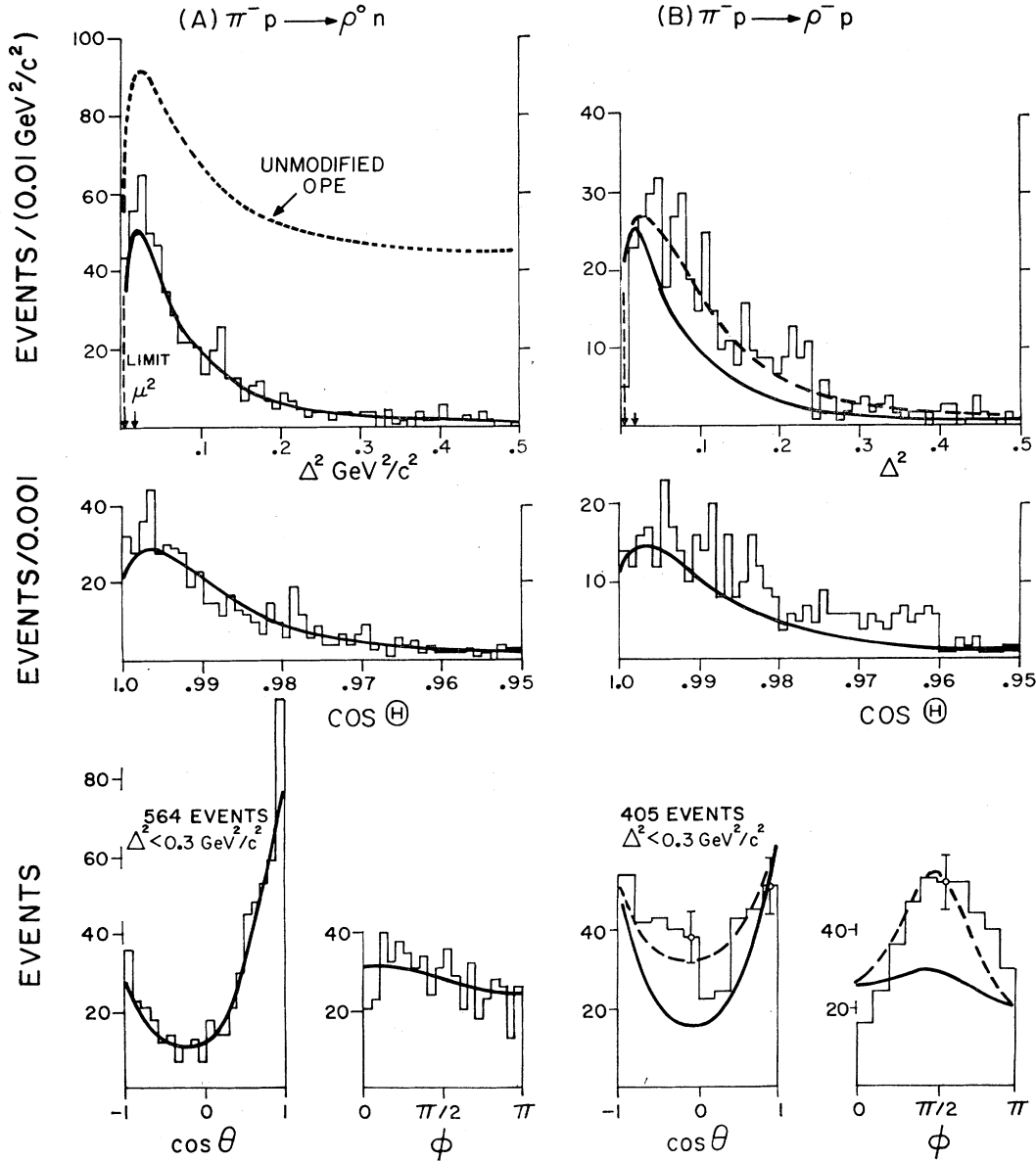


FIG. 2. Various differential cross sections for the ρ^0 and ρ^- (defined here by 0.72–0.84 GeV). Plotted are the $-t = \Delta^2$, $\cos\Theta$ ($\Theta =$ total c.m. scattering angle), $\cos\theta$, and ϕ distributions for the ρ^0 and ρ^- . The results of the AOPE model are shown as solid curves. In the case of the ρ^- , the result of the ω -exchange addition (see text) is indicated with dashed curves.

in the region $m_{\pi\pi} < 1.4$ GeV, $-t < 0.3$ GeV $^2/c^2$]. The above t cut is made in accord with the data which show a change in t distribution near $-t \approx 0.3$ (GeV/c) 2 from a sharp to a relatively flat distribution for the entire dipion mass range.

Thus the total amplitude for the reactions (1) and (2) in our model consists of pion-exchange and nucleon-pole terms (NPT), both of which are properly absorption modified, i.e.,

$$\langle \mu\lambda' | T | \lambda \rangle = \langle \mu\lambda' | A | \lambda \rangle + \langle \lambda' | T_{\text{NPT}} | \lambda \rangle. \quad (3)$$

Explicit helicity amplitudes of the pion-exchange terms

for the dipion in S , P , and D waves are given in Appendices A and B, and nucleon-pole terms are given in Appendix C. $(\mu\lambda', \lambda)$ in Eq. (3) refer to the helicities of the dipion, outgoing, and incoming nucleons, respectively. The pion-exchange term can be written in the form [Eq. (A3) of Appendix A]

$$\langle \mu\lambda' | A | \lambda \rangle = \sum_l \sum_I \langle \mu\lambda' | A_l^I | \lambda \rangle Y_l^\mu(\theta, \phi),$$

$$\langle \mu\lambda' | A_l^I | \lambda \rangle = (m_{\pi\pi}/k) C^N C^I [\eta_l^I \exp(2i\delta_l^I) - 1] f_{\mu\lambda'\lambda}(s, t), \quad (4)$$

where l and I refer to the partial wave and isospin of the dipion; (θ, ϕ) are $\pi\pi$ scattering angles; (δ_l^I, η_l^I) are $\pi\pi$ phase shifts and inelasticities; $\sqrt{s} = m_{\pi\pi}$ refers to the dipion mass, and $k = (\frac{1}{4}s - m_\pi^2)^{1/2}$; C^I and C^N are isospin coefficients for the dipion and nucleon vertices, respectively. $f_{\mu\lambda}(s, t)$ gives the t dependence of the amplitudes which, in general, differ for different helicities. [In the unmodified model, $\sum |f_{0\lambda\lambda}|^2 \propto -t/(t - m_\pi^2)^2$.] Other constants are absorbed in $f_{\mu\lambda}(s, t)$. See Appendices A and B for details.

The cross section for the reactions (1) and (2) with the above amplitudes is (k_L = incident laboratory momentum)

$$\frac{d^4\sigma}{dm_{\pi\pi} d\theta d\phi} = \frac{1}{256\pi^2} \frac{k}{k_L^2} \frac{1}{2} \sum_{\mu\lambda\lambda'} |\langle \mu\lambda' | T | \lambda \rangle|^2. \quad (5)$$

The cross section in the form of (5) and (3) is suitable for the analysis of the reactions (1) and (2), particularly for the $\pi\pi$ system, as the above set of four independent variables completely describes the reactions. (Any five-point vertex function needs five independent variables; the total c.m. energy is the fifth variable.) Thus a set of $\pi\pi$ phase shifts predicts the dipion mass spectra and $\cos\theta$ distributions as a function of dipion mass for the reactions (1) and (2). The ϕ and t distributions are not very sensitive to a choice of phase shifts, except in the peak regions of the ρ and the f , whereas the combined $\cos\theta$ - ϕ distributions are quite useful for the cases of high statistics. We also comment that the amplitudes of the nucleon-pole terms in (3) must be expressed in terms of the above set of four variables.

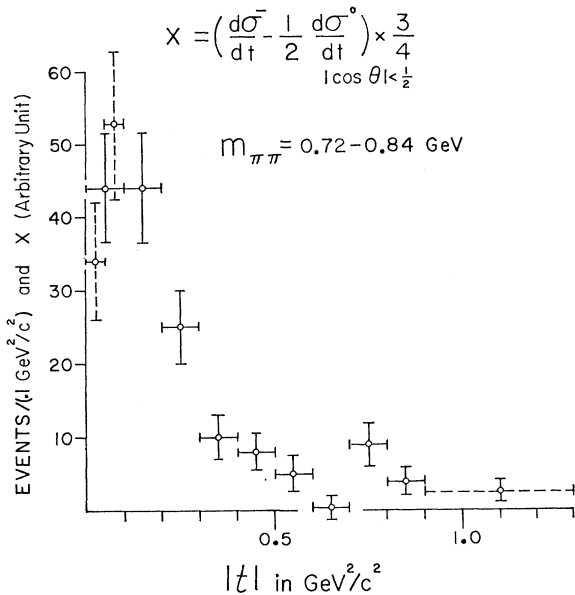


FIG. 3. Cross-section combination $X = (d\sigma/dt) (\pi^- p \rightarrow \rho^- p) - \frac{1}{2}(d\sigma/dt) (\pi^- p \rightarrow \rho^0 n)$. This combination is approximately equal to the ω -exchange contribution to the ρ^- production. In order to bring out the dominant helicity states due to ω exchange (which gives a $\sin^2\theta$ distribution), we took the data for $|\cos\theta| < \frac{1}{2}$ and made a correction for the rest of $\cos\theta$.

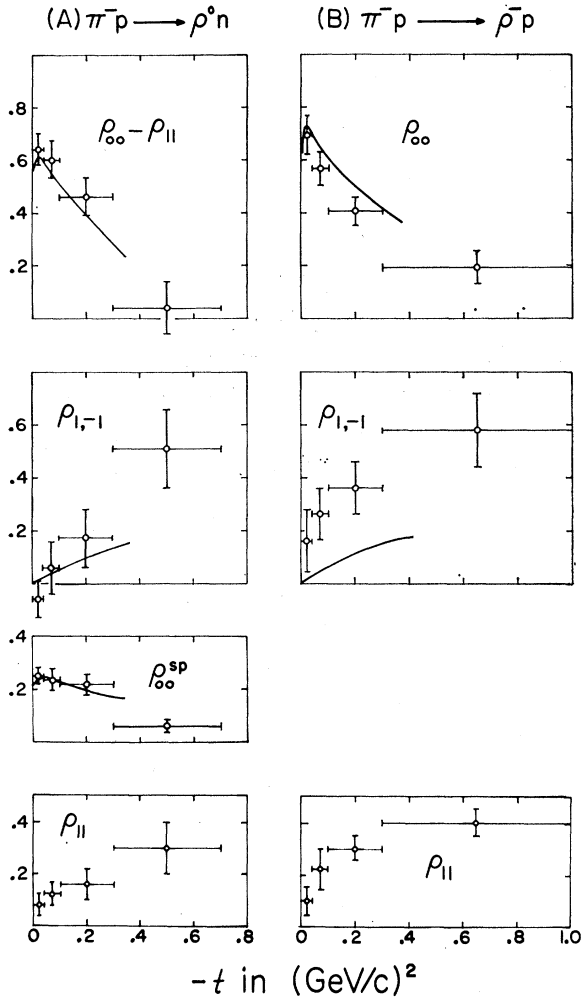


FIG. 4. Density-matrix elements of the ρ^0 and ρ^- (0.72-0.84 GeV). The solid curves are the AOPE calculations weight averaged over the mass region. (In the case of the ρ^- , only the π -exchange contribution is shown.)

This program is carried out in Appendix C, together with an appropriate correction for the absorption in the entrance and exit channels.

ρ Meson

To test the cross section (5) against experimental data, we have chosen the peak region of the ρ (0.72-0.84 GeV) and tried the set of S - and P -wave phase shift given by Walker *et al.*² For each of the 20- or 40-MeV mass bins, we vary the t values in finite steps and calculate $\cos\theta$ - ϕ distributions and compare various projections or two-dimensional distributions of the variables of Eq. (5). The resulting $\cos\theta$ - ϕ distribution (summed over for $m_{\pi\pi}$ and t) showed a reasonable accord with the data.

The results of the absolute cross-section calculations

$$d\sigma/d\cos\theta, d\sigma/d\phi, \text{ and } d\sigma/d\phi$$

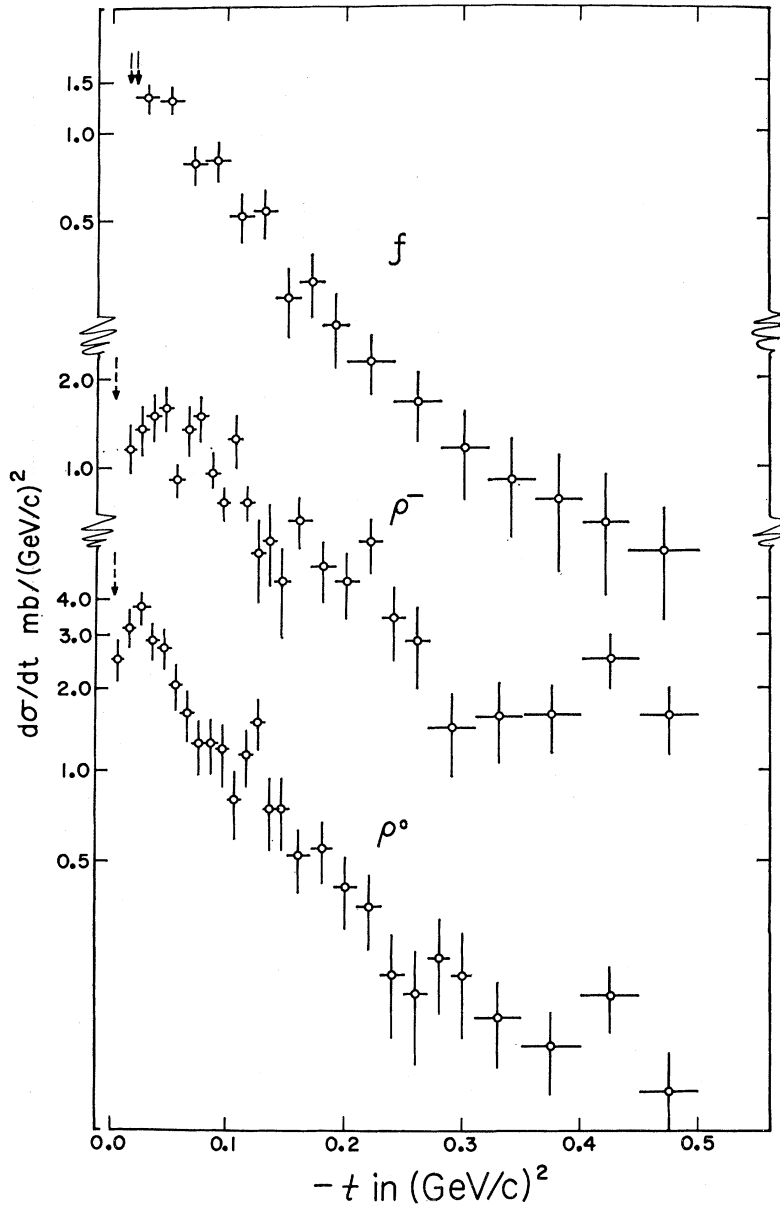


FIG. 5. $d\sigma/dt$ for ρ^0 , ρ^- , and f production. Kinematic limits are indicated by arrows.

thus obtaining for the peak region of the ρ for reactions (1) and (2) are compared with the data in Fig. 2. The $\cos\theta$ (θ = total c.m. scattering angle) distribution has an advantage over a t distribution for small t or $\cos\theta\sim 1$, but is otherwise equivalent. The phase shifts for the solid curves in Fig. 2 are those of Walker *et al.*² for the S waves, and P -wave phase shift corresponding to a Breit-Wigner resonance shape with

$$\begin{aligned} m(\rho^0) &= 775 \text{ MeV}, & \Gamma(\rho^0) &= 140 \text{ MeV}, \\ m(\rho^-) &= 770 \text{ MeV}, & \Gamma(\rho^-) &= 135 \text{ MeV}, \end{aligned} \quad (6)$$

and the errors are of the order of 10 MeV. In case of the ρ^0 , the over-all agreement is quite remarkable, with

the exception of the sharp spike near $\cos\theta=1$, which is not reproduced in our calculation. This serves to remind us that there are still some processes (such as extremely peripheral production of N^* 's) we have left out. For the ρ^- all the features of the data require ω exchange in addition to π exchange. A crude estimate of the Regge ω -exchange contribution based on (i) the cross-section combination of the form

$$(d\sigma/dt)(\rho^-) - \frac{1}{2}(d\sigma/dt)(\rho^0) \quad (7)$$

as suggested by Contogouris *et al.*¹⁷ and (ii) the assump-

¹⁷ A. P. Contogouris, J. Thanh Van, and H. J. Lubatti, *Phys. Rev. Letters* **19**, 1352 (1967).

tion that ω exchange gives only helicity ± 1 states of the ρ^- (with no interference with the π -exchange process, and neglecting other exchanges) can explain the data rather well. We show in Fig. 3 the cross-section combination, Eq. (7), for the dipion mass region 0.72–0.84 GeV.¹⁸ Figure 2 shows the effect of the ω exchange isolated as above, superimposed (dashed curves) on the AOPE, NPT results (solid curves).

It becomes clear now that the inclusion of the nucleon-pole terms certainly improves the over-all analysis of the data in the ρ region. The off-mass-shell correction of the form (A12) also helped to bring the agreement in the t distribution. The normalization of $\sigma_{\pi\pi}$ with the ρ peak as $\sigma_{\pi\pi} \approx 12\pi/k^2$ is not essential, although our result certainly justified the normalization. One further remark can also be made, which is that

extreme care must be exercised when the $\cos\theta$ distribution in the t region, $|t| > 5m_\pi^2$, is used to deduce the $\pi\pi$ phase shift in the nonabsorptive type of model owing to the ever-increasing proportions of nonzero helicity state in the high- $|t|$ region.

We show in Fig. 4 the density-matrix element for the ρ using the parametrization of $I(\cos\theta, \phi)$ given in Eq. (A11) of Appendix A, together with the absorption-model results (solid curves) weight averaged over the mass region 0.72–0.84 GeV. The experimental data of $\rho_{11}/(\rho_{00}+2\rho_{11})$ for the ρ^- production are simply obtained from the normalization condition $\rho_{00}+2\rho_{11} \approx 1$, whereas for the ρ^0 production, we use

$$\frac{\rho_{11}}{\rho_{00}+2\rho_{11}} = \frac{1}{3} \left(1 - \frac{\rho_{00}-\rho_{11}}{1-\rho_{00}^S} \right). \quad (8)$$

We use the calculated value of ρ_{00}^S from the S -wave phase shifts and AOPE model, $\rho_{00}^S \approx 0.15-0.20$, as ρ_{00}^S cannot be directly isolated from the data.

The one-pion-exchange dominance for the production of the ρ^0 for $-t < 0.3$ (GeV/c)² is quite apparent from the t dependence (and the beam-momentum dependence of the ρ^0 production; see below). Further, we have shown that the total amplitude in the form of (3) and (4) is quite capable of reproducing important features of the ρ^0 (and of the ρ^- when we include the ω -exchange contribution in addition). We also point out, in the light of current interest of the Reggeized π exchange,¹⁹ that our data indicate no deviation from the “turnover” of $d\sigma/dt(\pi^-p \rightarrow \rho^0n)$ below $-t < m_\pi^2$ consistent with an evasive solution,²⁰ and in contrast to the data of Selove *et al.*²¹ While the data also suggest possible nonzero ρ_{11} even near $-t_{\min}$ ($\sim 0.2m_\pi^2$), its relation with a possible pion conspiracy¹⁹ or Regge cuts must await further theoretical clarifications. ρ_{11} is expected to be small but nonzero in the absorption model when the lowest partial waves of the entrance and exit channels are completely absorbed.

In closing this section, we show in Fig. 5 the t distributions of $\rho^{0,-}$ and the f^0 , where we indicate the kinematic limit of t by dashed arrows. A similarity of ρ^0 and f^0 distributions is particularly apparent in contrast with the ρ^- . In Fig. 6 are shown the cross sections for the reactions $\pi^-p \rightarrow \rho^0n$, ρ^-p , and fn . The ρ^0 and f production follows a P_{lab}^{-2} dependence rather well, whereas ρ^- production deviates from such a dependence.

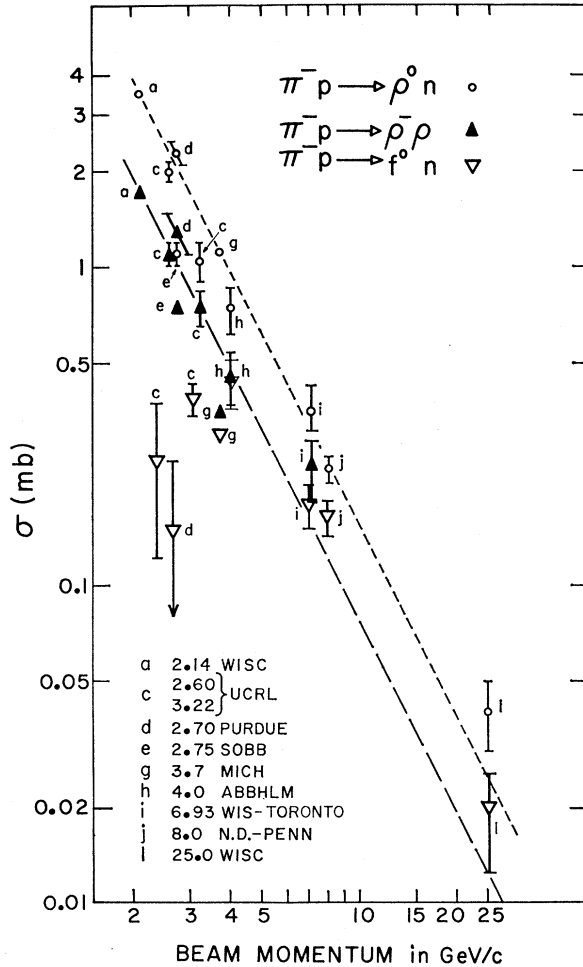


FIG. 6. Beam momentum dependence of the cross sections for ρ^0 , ρ^- , and f production. The dashed lines show P_{lab}^{-2} dependence.

¹⁸ In order to bring out ± 1 helicity states of the ρ we limited ourselves to the region of $\cos\theta$, $|\cos\theta| < 0.5$, with a correction for other region of $\cos\theta$, assuming a $\sin^2\theta$ distribution.

¹⁹ See a theoretical review by L. Bertocchi, in *Proceedings of the Heidelberg Conference on Elementary Particles, 1967* (Wiley, New York, 1968). See also L. Durand III, *Phys. Rev. Letters* **19**, 1345 (1967).

²⁰ Our data on $\rho_{00}(d\sigma/dt)$ for the ρ^0 agree very well with the model of S. Frautschi and L. Jones, *Phys. Rev.* **164**, 1918 (1967). The data also agree with the ρ^+ data of M. Aderholz *et al.*, *Phys. Letters* **27B**, 174 (1968). G. V. Dass and C. D. Froggatt [*Nucl. Phys.* **B8**, 661 (1968)], in their Regge-pole analysis, however, favor a conspiracy solution.

²¹ W. Selove, F. Forman, and H. Yuta, *Phys. Rev. Letters* **21**, 952 (1968).

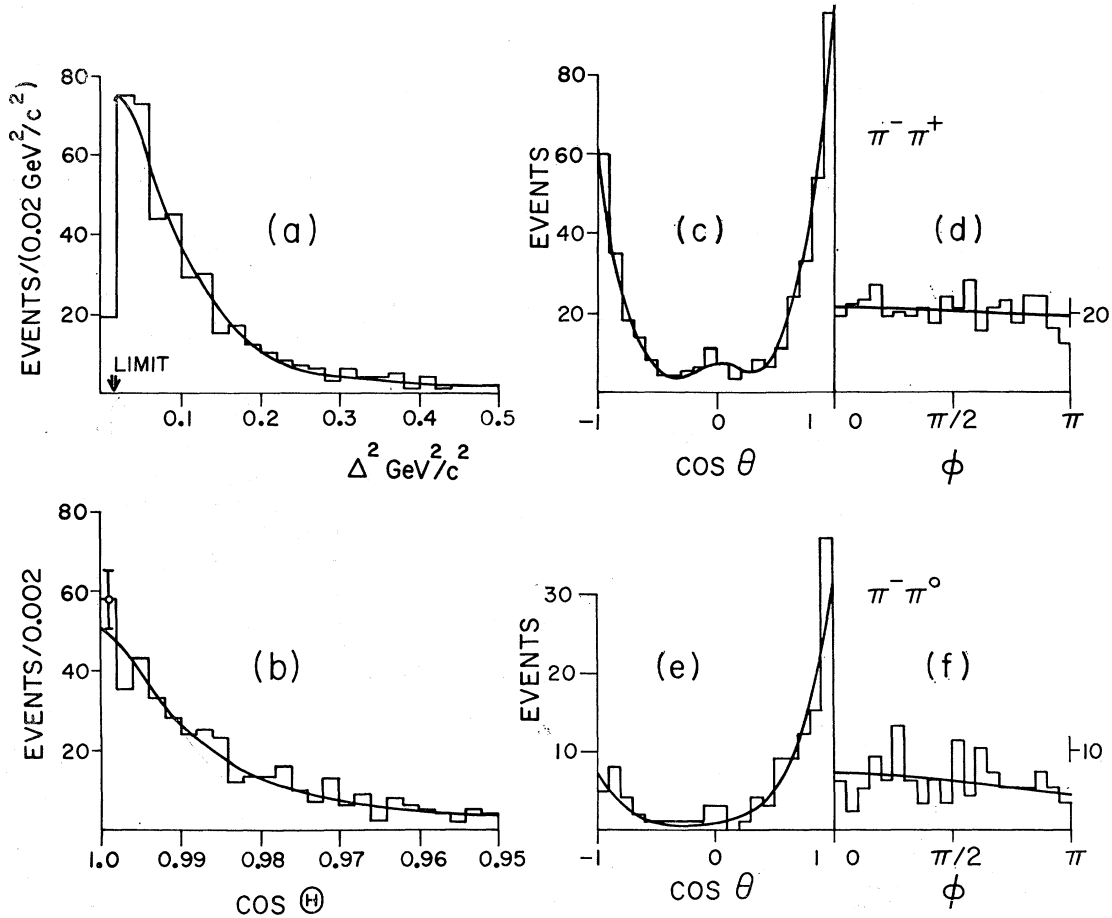


FIG. 7. Various differential cross sections for the f region, defined here as 1.21–1.33 GeV of dipion mass. The $-t$ and $\cos\Theta$ distributions for the f are shown in (a) and (b). Plotted in (c) and (d) are $\cos\theta$ and ϕ distributions of the f . Also, in (e) and (f) are plotted the $\cos\theta$ and ϕ distributions of the $\pi^-\pi^0$ state in the f region. The solid curves are the AOPE results discussed in the text.

III. RESULTS

f^0 -Meson Region

Previous absorption-model calculations¹⁵ by various authors of the f production, based on a simple assumption of no background and completely elastic D -wave $\pi\pi$ amplitude, have indicated that (i) the calculated cross section was too large, (ii) the calculated $d\sigma/dt$ was falling slower than the experimental data at large $|t|$, and (iii) the experimental $\cos\theta$ distribution shows near absence of events in the $\cos\theta \approx 0$ region, in gross disagreement with the density-matrix element of a pure D wave. An improvement in the analysis is readily made when we assume a small width of the f , together with some form factor, and some amount of S -wave scattering to account for the polar angle distribution near $\cos\theta \approx 0$. Furthermore, it is likely that the η_{D^0} (inelasticity of the $I=0$ D wave) is appreciably less than unity near and above the f peak region (see below). The mass spectra and $\cos\theta$ distributions of $\pi^-\pi^+$ and $\pi^-\pi^0$ states in the f region indicate the presence of some amount of P wave (or F wave) and $I=2$ D wave.

With the above preliminaries we study the f -meson and other nonresonant partial-wave amplitudes in the f region. We take a narrow dipion mass region, 1.21–1.33 GeV, as there is a considerable change in the $\cos\theta$ distributions below and above the f peak region. In Fig. 7 we show the distributions in t , $\cos\Theta$, $\cos\theta$, and ϕ for the $\pi^-\pi^+$ state, and $\cos\theta$ and ϕ distributions for the $\pi^-\pi^0$ state of the mass region under consideration. The variation with t of the joint $\cos\theta$ - ϕ distribution for the f is shown next in Fig. 8.

In carrying out the absorption-model calculations as outlined in Sec. I and the Appendices, we leave out higher partial waves, $l \geq 3$, assuming that they play a minor role (and in case of $I=1$ F wave, the g -meson signal indicates a negligible contribution in the f region). Since we expect the $I=0$ D wave to dominate the $\pi^-\pi^+$ state, we determine the approximate phase shift δ_{D^0} and inelasticity η_{D^0} as functions of dipion mass from the observed mass spectrum with various t cuts. It is seen that the shape of $d\sigma/dt$ is well reproduced by the absorption-modified OPE amplitudes. The magnitudes of the cross section and the inelasticity η_{D^0} is sensitive to the

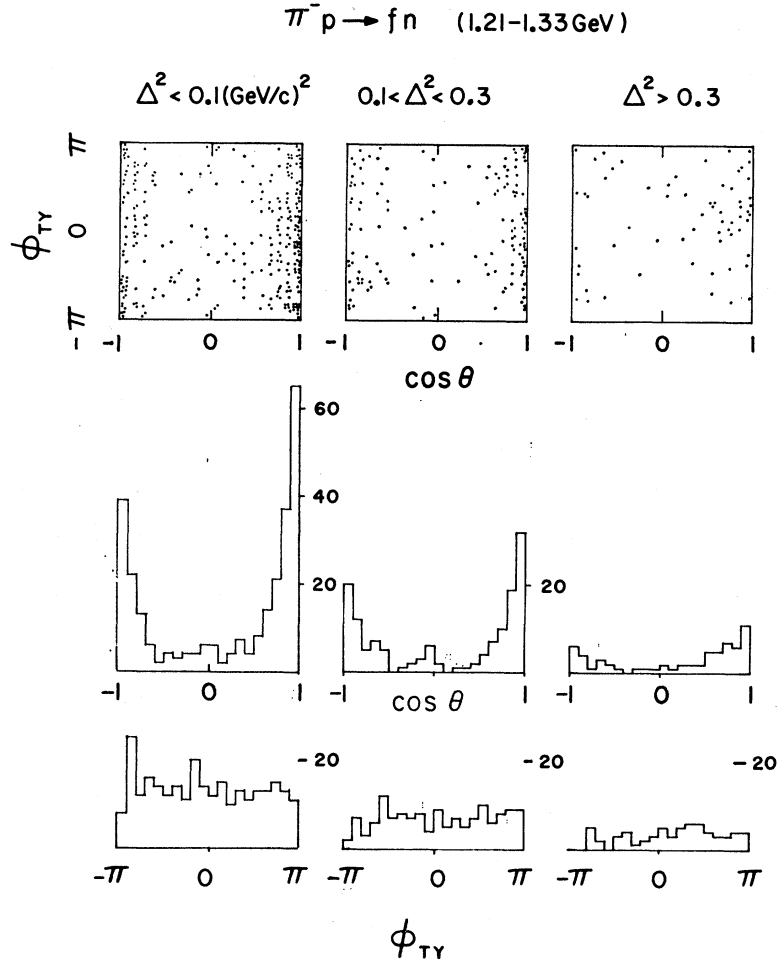


FIG. 8. Scatter plots of $\cos\theta$ - ϕ distributions for three different regions of $-t (= \Delta^2)$ and projections for the $\pi^-\pi^+$ state in the f region.

nucleon-pole terms and off-shell corrections. With the choice of the nucleon-pole terms and the Dürr-Pilkühn off-shell corrections, as used for the ρ^0 case, we obtain $\eta_D^0 \approx 0.6$ at the f peak, which implies a ratio $f \rightarrow \text{inelastic}/f \rightarrow \pi\pi \approx 0.25$. The average behavior of P -wave and $I=2$ D -wave amplitudes are then estimated from the asymmetry of the $\pi^-\pi^+$ angular distribution and the cross section of the $\pi^-\pi^0$ state. The $I=2$ D wave, in particular, is allowed to vary only within the bounds of our independent analysis²² of the reactions $\pi^- p \rightarrow \Delta^+ \pi^- \pi^-$ and $\pi^+ p \rightarrow \pi^+ \pi^+ n$. The S -wave amplitudes are adjusted to give the observed behavior near $\cos\theta \approx 0$ of the $\pi^-\pi^+$ state and the details of the $\pi^-\pi^0$ state angular distribution.

After a great number of trials with different sets of average δ 's and η 's covering the domain of reasonable sets of phase shifts (connecting smoothly with low-energy phase shifts), we find that the following set gives the best fit to the over-all behavior of the data ($\langle \rangle$ for

average):

$m_{\pi\pi}$ (GeV)	1.22	1.24	1.26	1.28	1.30	1.32
δ_D^0 (deg)	42	62	80	98	108	122
η_D^0	0.77	0.67	0.65	0.60	0.60	0.60

(9a)

$$\begin{aligned}
 \langle \delta_{S^0} \rangle &= 100^\circ, & \langle \eta_{S^0} \rangle &= 0.5, \\
 \langle \delta_{S^2} \rangle &= -23^\circ, & \langle \eta_{S^2} \rangle &= 0.8, \\
 \langle \delta_{P^1} \rangle &= 162^\circ, & \langle \eta_{P^1} \rangle &= 0.92, \\
 \langle \delta_{D^2} \rangle &= -5^\circ, & \langle \eta_{D^2} \rangle &= 1.0.
 \end{aligned}
 \tag{9b}$$

The curves in Fig. 7 correspond to the cross sections resulting from these. We suggest that, while (9) gives a likely set of phase shifts for the P and D waves, the uncertainties in the S -wave phase shifts are quite appreciable, owing to a low S -wave unitarity bound. For the resonance parameter of the f (see below for further confirmation), we obtain

$$\begin{aligned}
 \text{mass } &1275 \pm 10 \text{ MeV}, & \text{width } &120 \pm 15 \text{ MeV}, \\
 \text{cross section } && &0.21 \pm 0.06 \text{ mb.}
 \end{aligned}
 \tag{10}$$

²² R. Morse, A. F. Grafinkel, B. Y. Oh, W. D. Walker, P. Berenyi, J. Prentice, and N. R. Steenberg (unpublished).

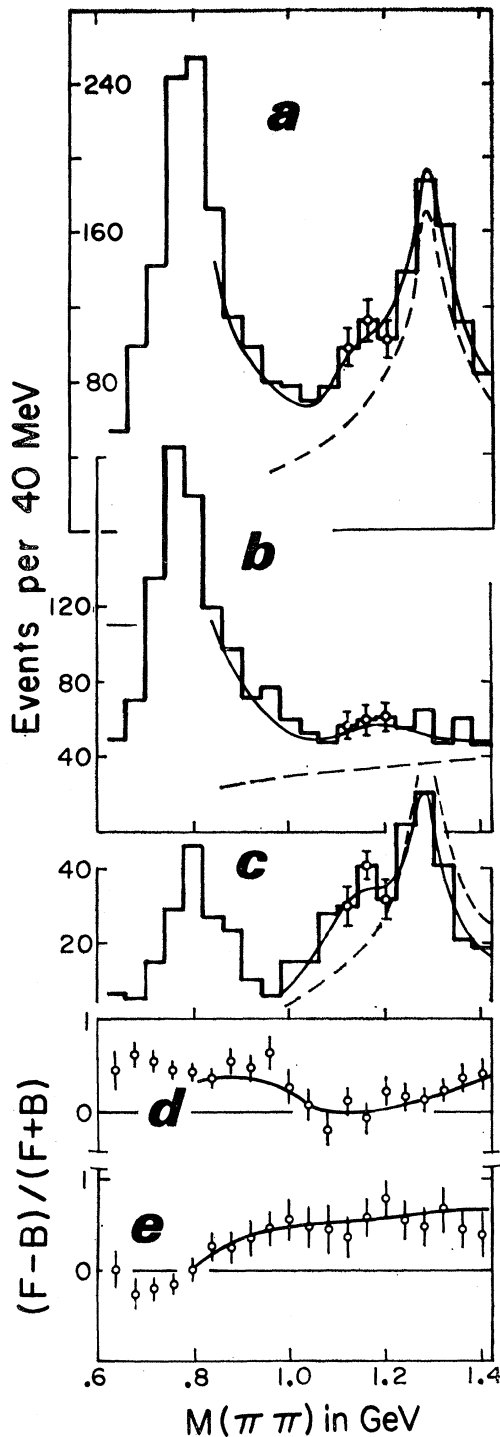


FIG. 9. Dipion mass spectra of (a) $\pi^-\pi^+$ and (b) $\pi^-\pi^0$. (c) $\pi^-\pi^+$ mass spectrum in the region $\cos\theta < -0.8$. (d) and (e) The ratio $(F-B)/(F+B)$ versus dipion mass for the $\pi^-\pi^+$ and $\pi^-\pi^0$ states. The solid curves are the result of our phase-shift analysis (see Fig. 11 and the text). The mass spectra which result when we leave out P -wave contributions are indicated by the dashed curves in (a)–(c).

It should be mentioned that while the values of the η 's are uncertain (up to 10–15%) in our analysis, the relative magnitude and phases of the partial waves should have been determined with much less uncertainty. We have also estimated the ratio $(f \rightarrow \text{inelastic}/f \rightarrow \pi\pi)$ independently from the reactions $\pi^-p \rightarrow \pi^-\pi^+\pi^-\pi^+\pi^+$ and $\pi^-p \rightarrow K_1^0 K_1^0 n$, with a result^{23,24}

$$(f \rightarrow \pi^-\pi^+\pi^-\pi^+)/ (f \rightarrow \pi^-\pi^+) = (7 \pm 2)\%,$$

$$(f \rightarrow K\bar{K}) / (f \rightarrow \pi\pi) = (6 \pm 2)\%. \quad (11)$$

While further studies are required to determine the ratio $f \rightarrow \text{inelastic}/f \rightarrow 2\pi$ directly (no data are as yet available for the ratios $f \rightarrow \eta\eta$, $\eta\pi\pi/f \rightarrow 2\pi$), the f meson

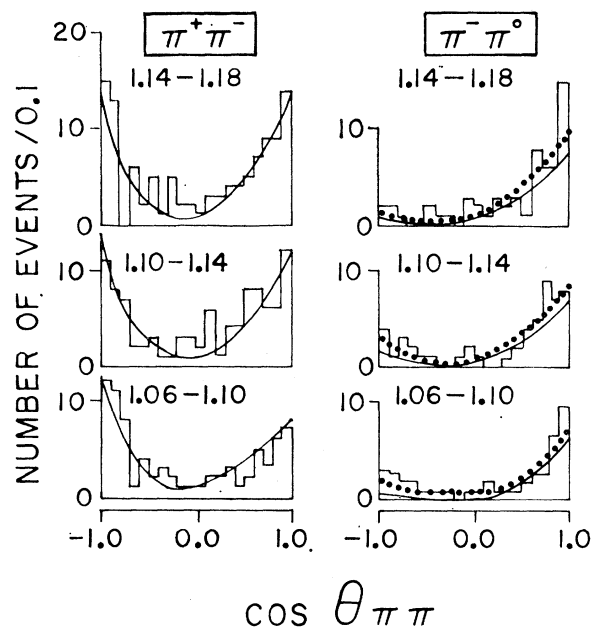


FIG. 10. The $\cos\theta$ distributions of $\pi^-\pi^+$ and $\pi^-\pi^0$ states in the 1.06–1.18-GeV region. The solid and dotted curves correspond to two solutions of phase shifts [see also Fig. 11(c)].

seems to show considerable inelasticity, and our value of $\eta_{D^0} \approx 0.6$ does not appear unreasonable.

1.0–1.2-GeV Region

The $\pi^-\pi^+$ mass spectrum and $\cos\theta$ distributions show some peculiar features around the 1.1–1.2-GeV region. We show in Figs. 9(a) and 9(b) the $\pi^-\pi^+$ and $\pi^-\pi^0$ mass spectra of reactions (1) and (2). An excess of events is seen in the 1.1–1.2-GeV region of the $\pi^-\pi^+$ system above what would be expected for a simple

²³ We use the peripheral data of Ref. 24 corrected for the beam momentum difference to estimate the $f \rightarrow K\bar{K}$ branching ratio. Our ratio is also consistent with the value given by Beusch *et al.* (Ref. 9). As for the ratio $f \rightarrow 4\pi/f \rightarrow 2\pi$, our results disagree with Ascoli *et al.* (Ref. 10), who imply 20% for $f \rightarrow 4\pi/f \rightarrow 2\pi$.

²⁴ D. J. Crennell, G. R. Kalbfleisch, K. W. Lai, J. M. Scarr, T. G. Schumann, I. O. Skillicorn, and M. S. Webster, Phys. Rev. Letters 16, 1025 (1966).

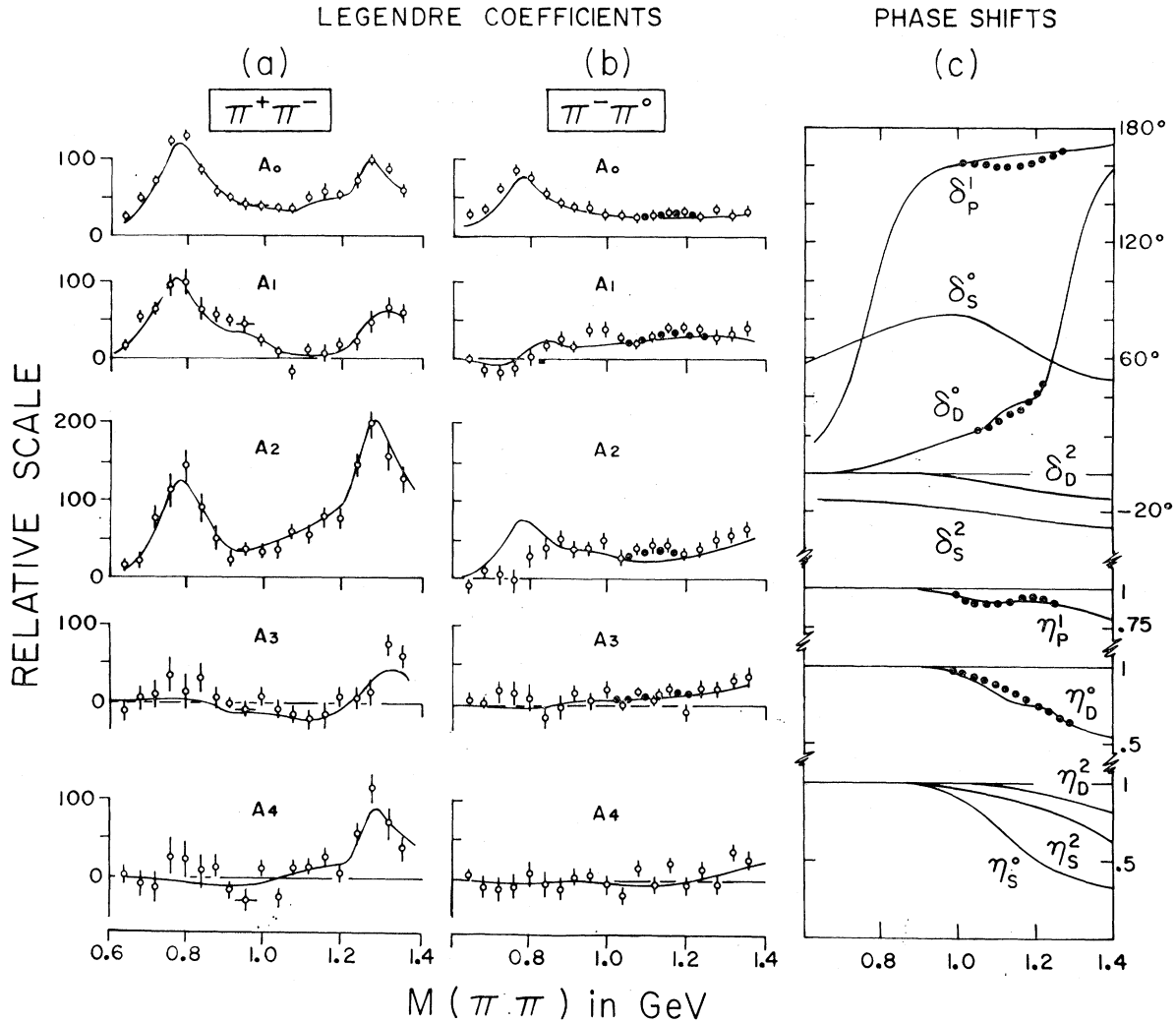


FIG. 11. (a) and (b) Legendre coefficients of $\cos\theta$ distributions for $\pi^-\pi^+$ and $\pi^-\pi^0$. (c) The results of the phase-shift analysis, as a function of $\pi\pi$ mass. The solid curves in (a) and (b) are the predictions of the phase-shift analysis shown as solid curves in (c). An alternative solution in the 1.0–1.2-GeV region and corresponding results are shown as dotted curves.

Breit-Wigner f meson. The signal is particularly enhanced in the region of $\cos\theta < -0.8$, as shown in Fig. 9(c). The variation of the $\cos\theta$ distribution with the dipion mass is shown in Fig. 10 for the $\pi^-\pi^+$ and $\pi^-\pi^0$ states. Also, in Figs. 9(d) and 9(e) are shown the corresponding $(F-B)/(F+B)$ ratio for the $\pi^-\pi^+$ and $\pi^-\pi^0$ states. The $\pi^-\pi^+$ enhancement in the 1.1–1.2-GeV region is clearly seen to be correlated with a rapid variation of the $\cos\theta$ distribution with $M(\pi^-\pi^+)$ and a lack of such variation for the $\pi^-\pi^0$ state. This variation has been observed in earlier studies.

A $\pi^-\pi^+$ enhancement in the 1.0–1.2-GeV region has been previously reported by Whitehead *et al.*²⁵ and Miller *et al.*²⁶ It is noted in Refs. 25 and 26 that the

observed enhancement has $I^G=0^+$ and J^P probably 2^+ and is not associated with the S^* , previously observed in the $K\bar{K}$ state.^{24,9} The enhancement is seen in the total $M(\pi^-\pi^+)$ of Ref. 25, but in Ref. 26 it is seen only for the region of $\cos\theta < -0.75$. The main results of our analysis in this mass region are given in an earlier publication.²⁷

The basic fact that one must consider is that the ratio $(F-B)/(F+B)$ becomes negative just above 1.0 GeV, and also that the anomaly in the mass spectrum shows mostly for $\cos\theta < -0.8$. Thus the effect observed is clearly the interference of two states or more of opposite parity. It could be the result of S - P or P - D or S - P - D interference. We observe, however, that the

²⁵ C. Whitehead, J. G. McEwen, R. J. Ott, D. X. Aitken, G. Bennett, and R. E. Jennings, *Nuovo Cimento* **53A**, 817 (1967).

²⁶ D. H. Miller, L. J. Gutay, P. B. Johnson, V. P. Kenny, and Z. G. T. Guiragossian, *Phys. Rev. Letters* **21**, 1489 (1968).

²⁷ B. Y. Oh, W. D. Walker, J. T. Carroll, M. Firebaugh, A. Garfinkel, R. Morse, J. D. Prentice, N. R. Steenberg, and E. West, *Phys. Rev. Letters* **23**, 331 (1969).

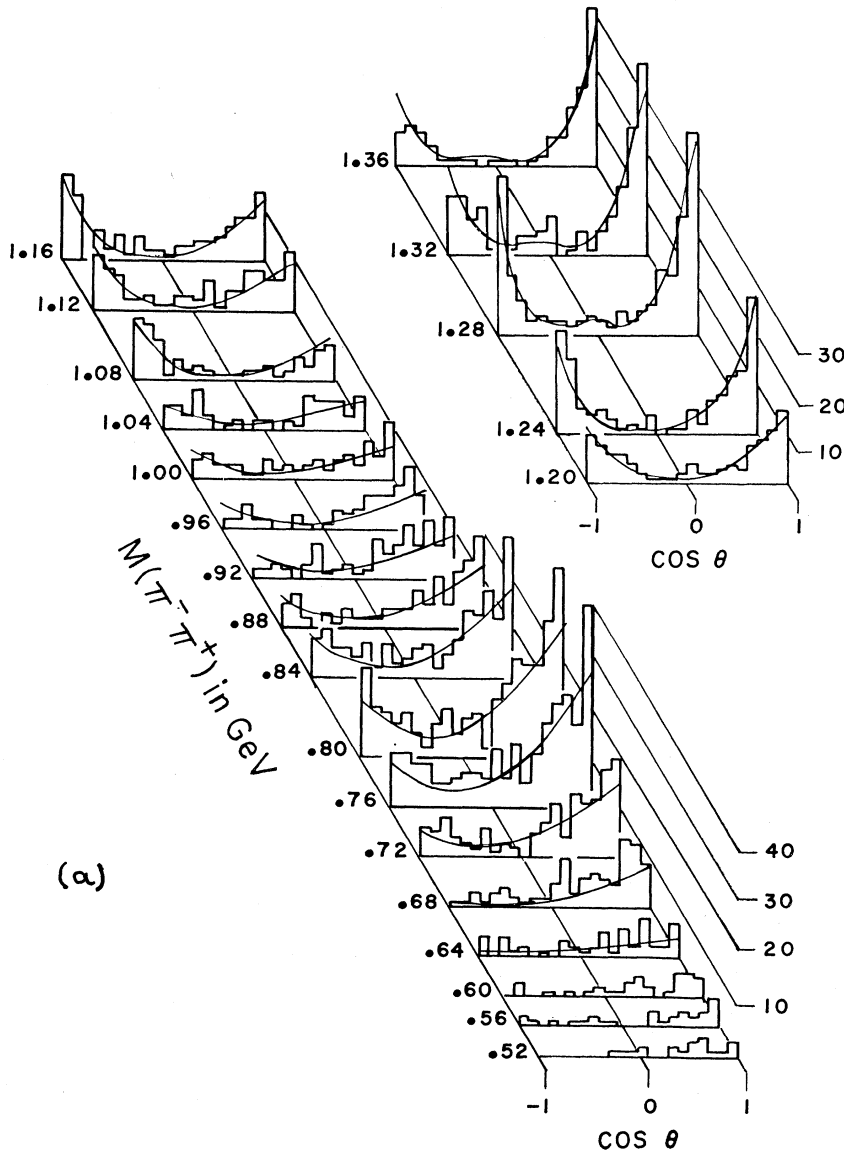


FIG. 12. (a) The $\cos\theta$ distributions versus $M(\pi^-\pi^+)$ for 40-MeV bins of $M(\pi^-\pi^+)$ centered around the mass values indicated. The solid curves are the results of the AOPE model which correspond to the phase shifts of Fig. 11(c). (b) The $\cos\theta$ distributions versus $M(\pi^-\pi^0)$. The solid curves correspond to the phase shifts of Fig. 11(c).

data²⁴ on the reaction $\pi^- p \rightarrow K_1^0 K_1^0 n$ indicate a strong absorption of the $I=0$ S wave in the process $\pi^-\pi^+ \rightarrow K\bar{K}$ near 1.1 GeV. Thus it seems almost certain that the amplitude vector of the $I=0$ S wave in the Argand diagram points near the center of the unitarity circle, leaving little room for large variation. Furthermore, since the backward peak must come from the real part of the amplitude, it is very difficult to see how S - P interference could possibly give the observed effect. The result is that the backward bump is almost certainly the result of P - D interference.

The angular distributions are also consistent with this interpretation. The backward hemisphere is always more sharply peaked than the forward hemisphere for the $\pi^-\pi^+$ state in the 1.1–1.2-GeV region as may be seen in Fig. 10. The same result is observed from examining

coefficients of the Legendre expansion of the $\cos\theta$ distributions, which are shown in Figs. 11(a) and 11(b) for the $\pi^-\pi^+$ and $\pi^-\pi^0$ states. The negative A_3 coefficient, which is present only in the 1.0–1.2-GeV region, indicates P - D interference.

In applying our phase-shift analysis to the 1.0–1.2-GeV region, we have all the problems we have faced for the case of the f region. In addition, a relatively diminished role of the dominant amplitude brings in some additional freedom in our choice of phase shifts. We are guided, however, by the following boundary conditions of the a_l^I 's: (i) We have to consider five partial-wave amplitudes, i.e., a_S^0 , a_S^2 , a_P^1 , a_D^0 , and a_D^2 (neglecting $l \geq 3$ waves); all of these may be partially inelastic. (ii) From the $\cos\theta$ distribution of the $\pi^-\pi^0$ state and from the expected behavior of a_P^1 which has passed

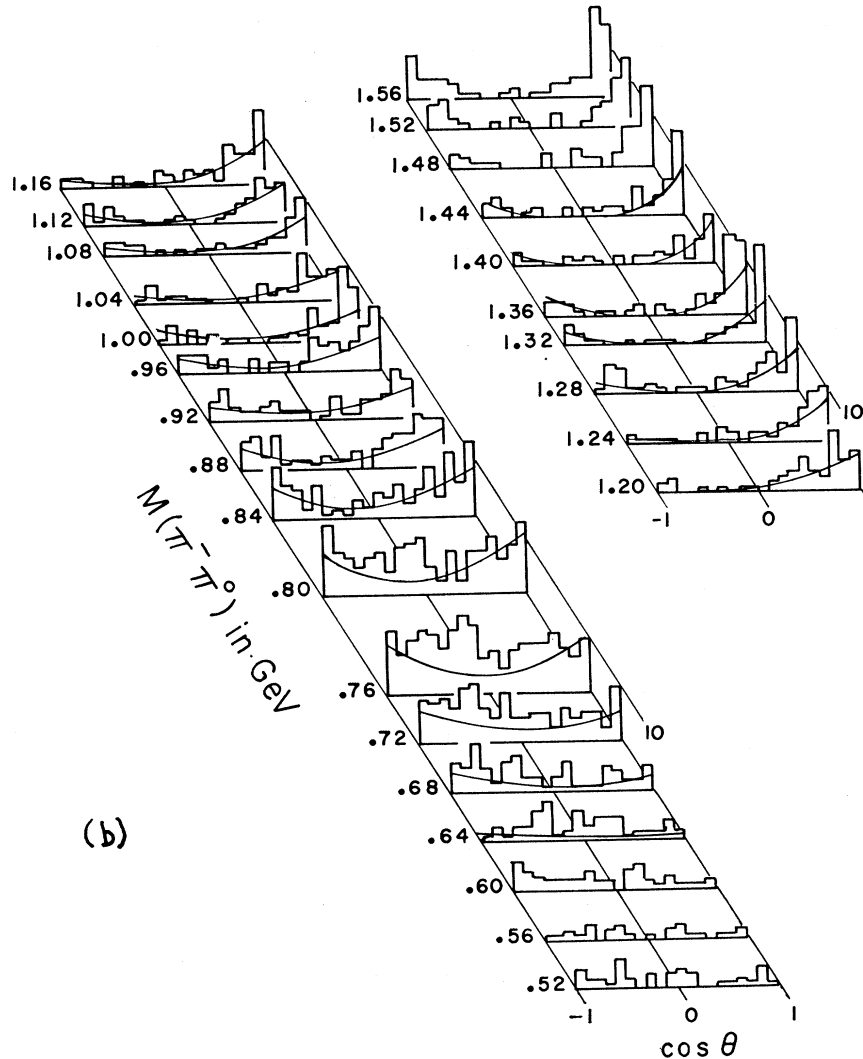


Figure 12. (Continued)

resonance ($\delta_{P^1} > 90^\circ$), the phase shift δ_{D^2} should be small and negative. δ_{S^2} is also expected to be small and negative, assuming no rapid variation of δ_{S^2} from its behavior below 1 GeV². Independent evidence of the small phase shifts for the $I=2$ waves comes from a study of reactions $\pi^- p \rightarrow \Delta^+ + \pi^- \pi^-$ ²² and $\pi^+ p \rightarrow \pi^+ \pi^+ n$. (iii) δ_{D^0} is expected to be positive, growing rapidly to reach 90° close to the f^0 -meson peak. (iv) The $I=0$ S -wave amplitude is an open question. The difficulty is mainly owing to its low unitarity bound, which makes the angular distribution rather insensitive to the choice of the S -wave amplitude. (v) The amplitude vectors in the Argand diagram of the important opposite-parity waves must be widely separated to give the observed negative $(F-B)/(F+B)$ ratio of the $\pi^- \pi^+$ state.

With the above boundary conditions of the a_l^I 's, we have tried a great number of possible sets of phase shifts to fit the observed cross section $\partial^2 \sigma / \partial m_{\pi\pi} \partial \cos \theta \partial \phi$. We have tested in particular the hypotheses of (a) D -wave

resonance (loop or cusp) with other waves varying slowly; (b) $I=0$ S -wave resonance rapidly sweeping the unitarity circle with other waves varying slowly (δ_{D^0} varying according to the Breit-Wigner formula); (c) a constant P -wave phase shift of 150° – 155° and $\eta_{P^1} = 0.8$ – 1.0 , with other waves varying slowly (δ_{D^0} varying according to the Breit-Wigner formula); and (d) a resonant P wave (loop) near the phase shifts given in (c) above.

Hypothesis (b) gives no solution; i.e., the observed anomaly is too large an effect to be caused by an S -wave amplitude. Hypothesis (a) is a very likely possibility. There are indications of an $I=0$ anomaly from data on charge exchange ($\pi^- + \pi^+ \rightarrow \pi^0 + \pi^0$). This would indicate that hypothesis (a) should be taken very seriously. We show this possibility in Fig. 11(c). We do not see a loop in the Argand diagram but rather a rapid growth in the $I=0$ D -wave amplitude.

We also find a solution in hypothesis (c) or (d) which

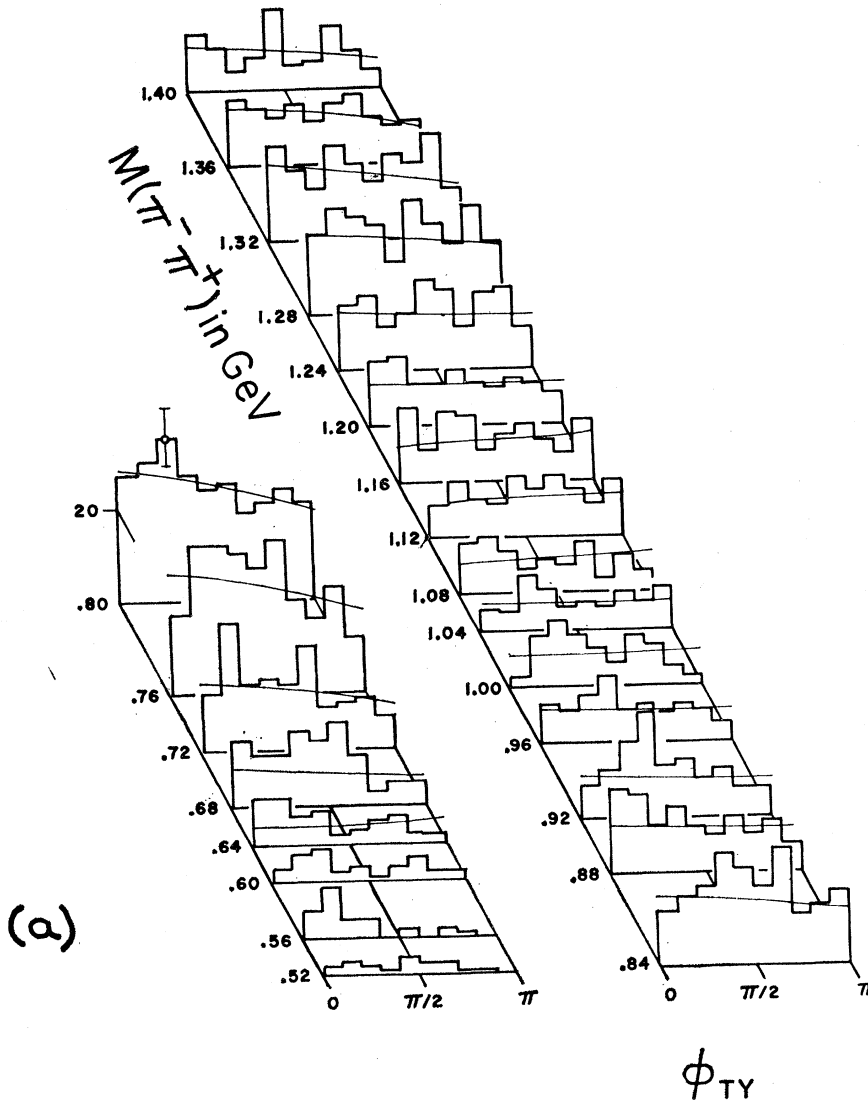


FIG. 13. (a) The ϕ distributions versus $M(\pi^-\pi^+)$ for 40-MeV bins of $M(\pi^-\pi^+)$ centered around the mass values indicated. The solid curves correspond to the phase shifts of Fig. 11(c). (b) The ϕ distribution versus $M(\pi^-\pi^0)$. The solid curves correspond to the phase shifts of Fig. 11(c).

gives an over-all agreement with the data. Our analysis is at the very least consistent with the existence of a ρ' . There can be no doubt that there is a very sizable P -wave amplitude present in the f^0 region. Whether or not this amplitude actually produces a loop²⁸ in the Argand diagram will have to wait on further analysis of inelastic channels such as $K\bar{K}$ or $\omega^0\pi$. The results are interesting in that they are similar in nature to the ρ region where there is a large $I=0$ S -wave amplitude which interferes with the ρ^0 .

The sets of phase shifts for solutions (a) and (d) are shown in Fig. 11(c) as solid and dotted curves (where the two solutions differ). The predictions of these solutions are shown as the smooth curves on Figs. 9-11

²⁸ If the P -wave amplitude resonates, its mass and width appear to be 1120_{-40}^{+100} and 150_{-50}^{+100} MeV, respectively. This agrees with the result of Regge-pole analysis by V. Barger and R. J. N. Phillips, Phys. Rev. Letters **21**, 865 (1968).

[again, where the predictions differ, solution (d) is shown as the dotted curves]. We have also shown as dashed curves in Figs. 9(a)-9(c) the dipion mass distributions which are expected when we leave out the P -wave amplitude completely while leaving everything else the same as for the solid curves. Thus, the P -wave amplitude, which accounts for the difference between the solid and dashed curves, is quite evident in the 1.1-1.2-GeV region.

The analysis in the 1.0-1.2-GeV region resolves in part the difficulties of determining the width of the f . It is not surprising that the mass and in particular the width of the f show such large differences in the literature, depending on how the "background" is treated. Furthermore, the inelastic P -wave amplitude may give rise to a part of the $\omega\pi$ enhancement in 1.0-1.2-GeV region (most likely apart from the B -meson production) producing the ambiguity in the analysis of the B

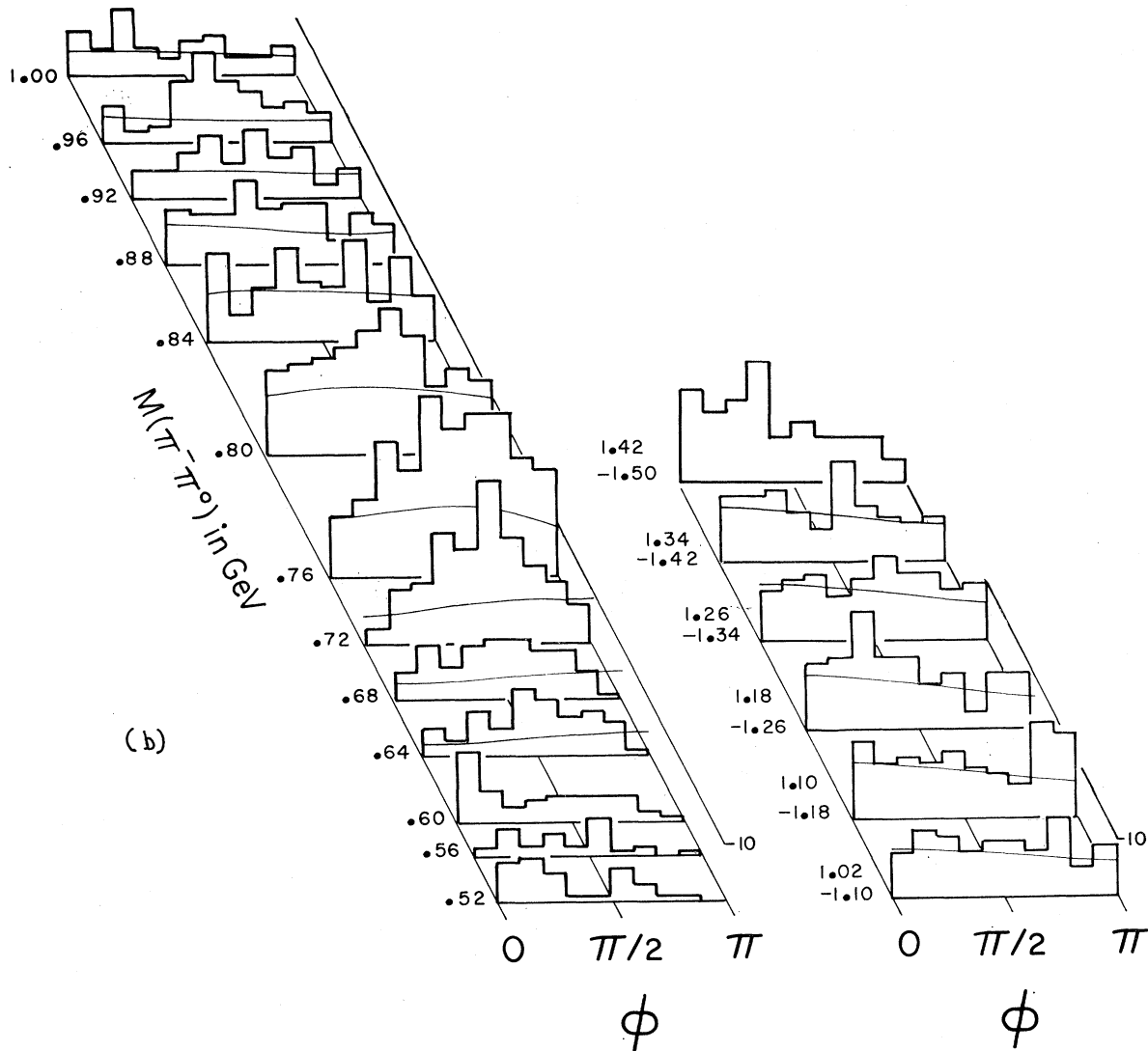


Figure 13. (Continued)

meson.²⁹ We also mention that the level of statistics of our data does not allow the unambiguous detection of a possible narrow resonance^{25,26} (≤ 40 MeV of width, particularly if it is an S -wave inelastic resonance) in the 1.0–1.1-GeV region.

Summary of Results

The set of phase shifts in other regions of dipion mass, which gives fits to the data up to 1.4 GeV, is summarized in Fig. 11(c). We have demanded a continuous and

smooth behavior of the phase shifts with energy. The absolute cross sections resulting from the above set of phase shifts are shown in Fig. 12 for $\cos\theta$, in Fig. 13 for ϕ , and in Fig. 14 for the $\cos\Theta$ distributions. The effects of $l \geq 3$ waves, which we have left out, become apparent in the $\cos\theta \approx -1$ region of $m_{\pi\pi} > 1.4$, since a combination of S , P , and D waves is not likely to produce the details of the observed angular distribution in the high-mass region. The $\pi^-\pi^+$ and $\pi^-\pi^0$ cross sections thus deduced are shown in Fig. 15. We estimate a systematic error of 15–20%.

IV. DISCUSSION

In our analysis of the $\pi\pi$ phase shifts we were forced to assume a simplified energy dependence for the partial scattering amplitudes. With greatly improved statistics, studies could be made of the hitherto unsuspected

²⁹ The B signal [Fig. 1(a)] shows extremely peripheral t distribution, quite similar to that of the f -meson production. The decay angular distributions, which vary rapidly with t , appear to show a mixture of 1^- , ..., and 1^+ , ..., series in our data. See M. Parkinson, Phys. Rev. Letters **18**, 270 (1967); M. Ademollo, H. R. Rubinstein, G. G. Veneziano, and M. A. Virasoro, *ibid.* **19**, 1402 (1968), for discussions on $\pi\pi \rightarrow \omega\pi$.

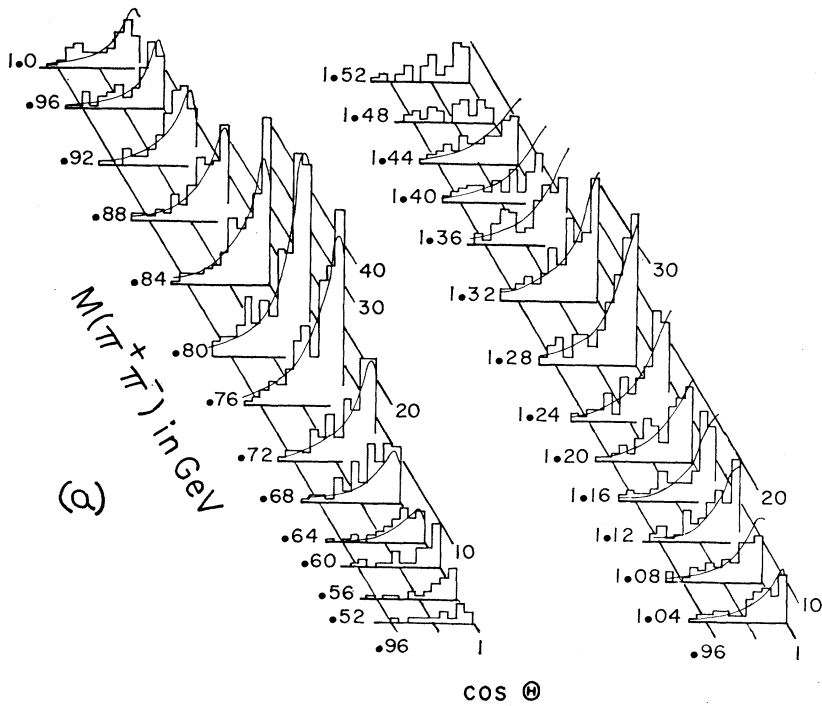
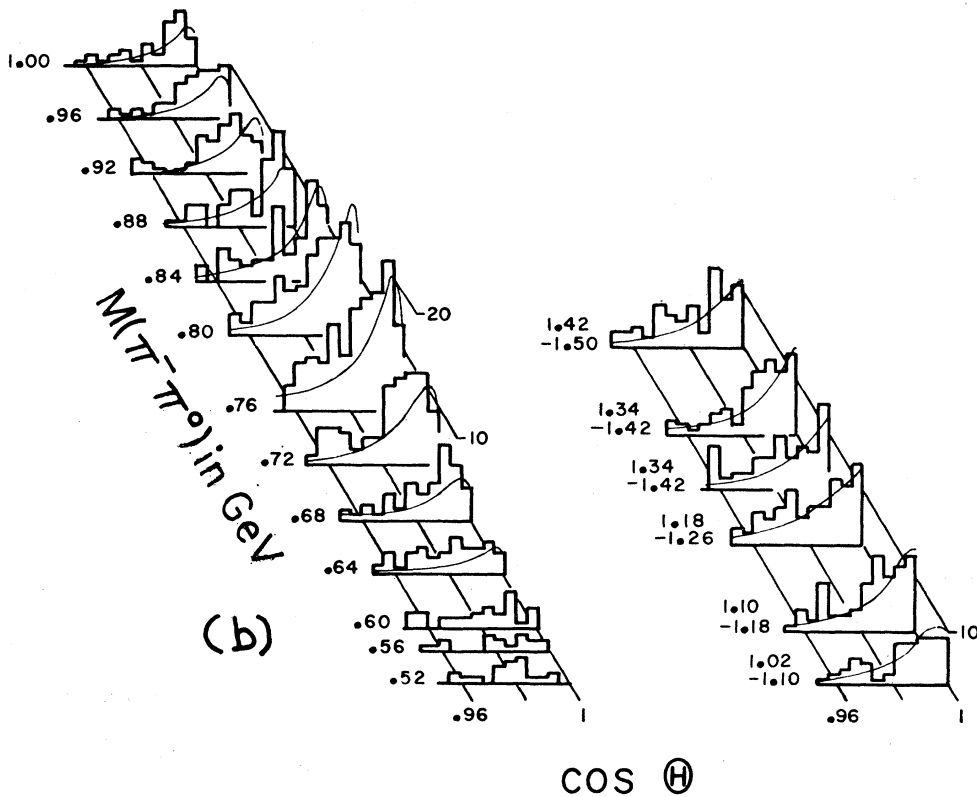


FIG. 14. (a) and (b) The c.m. cosine ($\cos\theta$) distributions versus $M(\pi^-\pi^+)$ and $M(\pi^-\pi^0)$, respectively (40-MeV bins of $\pi\pi$ mass unless otherwise indicated). The solid curves are the results of the AOPE model which correspond to the phase shifts Fig. 11(c).



behaviors of the partial-wave amplitudes. Further clarifications in the theoretical formalism are also needed, e.g., off-mass-shell correction, nucleon-pole terms, etc. These factors, in particular, affect the values of η 's, for which we estimate 10–15% of systematic errors in our analysis.

In the procedure used in our analysis, the errors of the $\pi\pi$ phase shifts become correlated, so that it is not really meaningful to assign an error to an individual point, but only to the curves. While large errors exist for the η 's (all the waves should be affected somewhat similarly; i.e., the correct values of the η 's should be larger

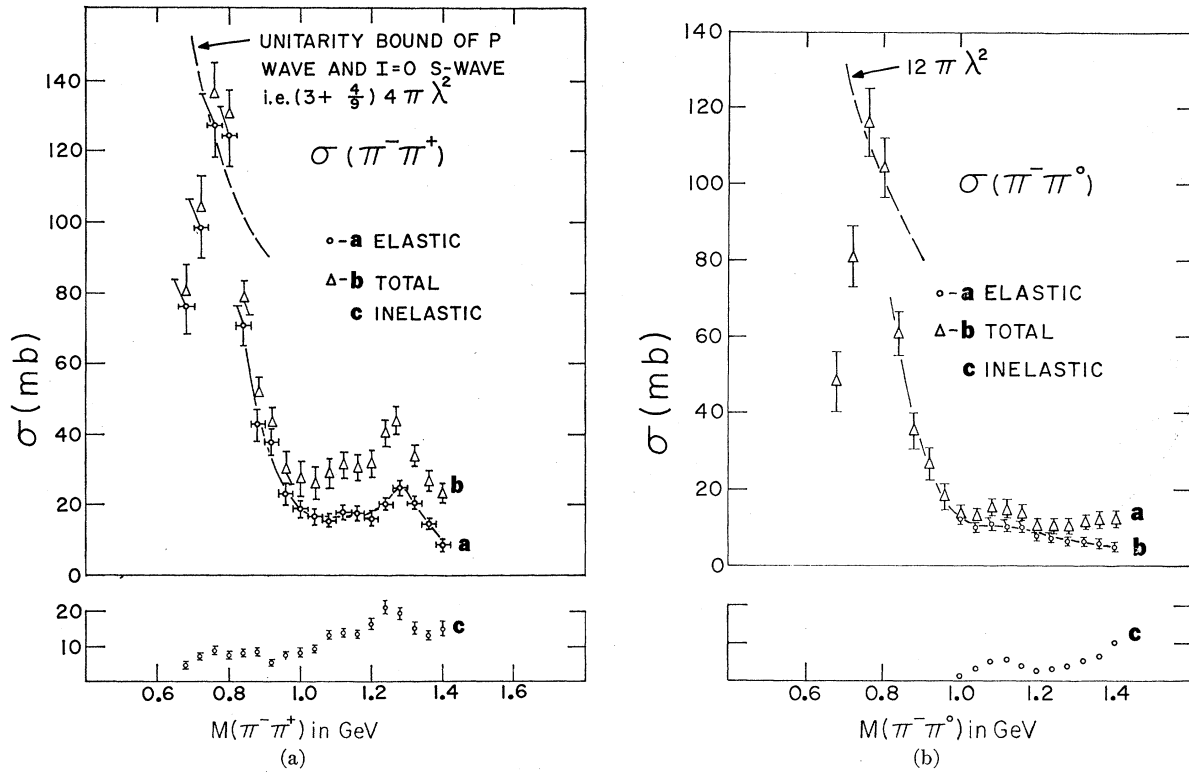


FIG. 15. (a) The $\pi^-\pi^+$ scattering cross section versus $M(\pi^-\pi^+)$ as deduced from our analysis. Elastic, total, and inelastic cross sections are shown. Total and inelastic cross sections include charge-exchange reaction $\pi^-\pi^+\rightarrow\pi^0\pi^0$. Elastic, total, and inelastic $\pi^-\pi^0$ cross sections versus $M(\pi^-\pi^0)$.

or smaller than the determined η 's, simultaneously), the main features of the relative magnitudes and phases of the important partial waves should have been correctly determined.

Our analysis shows that the reactions (1) and (2) in the region of small t and up to $m_{\pi\pi}\sim 1.4$ GeV can be described by the S -, P -, and D -wave $\pi\pi$ scatterings of the AOPE and NPT to a good approximation. Our estimate of the production of N^* 's in the kinematic region under consideration, which we have determined from the $\cos\theta^* < 0$ region of π^+n or π^0p [where θ^* is the p - n scattering angle in the π^+n/π^0p c.m. system; note that $\cos\theta^* < 0$ corresponds to $-t > 0.3$ (GeV/c)² for most of the πN mass], justifies our approximation.³⁰ Also consistent with our approximation is the very small cross section for the N^* production via $\pi^-p\rightarrow\pi^0N^*$.

The inelasticity of the f meson, which is found from our analysis using the absorption-modified one-pion-exchange model, seems reasonable when we compare with some of the inelastic channels directly observed. Finally, our analysis indicates the important role of the P -wave amplitude in the 1.0–1.2-GeV region and its interference with D and S waves. The statistics of our data do not allow further studies of possible resonance behavior for the D -wave or P -wave amplitude.

One might argue against the existence of a P -wave resonance because of the photoproduction data^{31,32} on π pairs in the 1.0–1.5-GeV/c² mass range. Our data and analysis both indicate a very weak coupling of the possible ρ' to the π - π channel. In amplitude a ρ' could be at most $\sim 10\%$ the size of the ρ in the π - π channel in terms of the relative diameter of the loops in the Argand diagram (Fig. 16). Thus, the experiment must have really good statistics to detect the ρ' in the photo experiments. As mentioned previously, the existence of a large P -wave amplitude is certain. It is interesting that the f^0 region is very similar to the situation in the ρ region in which the dominant $I=1$ amplitude interferes with the $I=0$ S -wave amplitude. In the f^0 region the dominant $I=0$ D wave amplitude interferes with the $I=1$ P wave amplitude. The resonances ϵ and ρ' would be consistent with Veneziano's dual representation.³³ It also seems that there may be some structure in the $I=0$ D wave in the form of a rapid change in the phase shift below the f^0 . This would be indicative of perhaps two nearly resonant amplitudes in the $I=0$ D wave.

³¹ N. Nicks, A. Eisner, G. Feldman, L. Litt, W. Lockeretz, F. Pipkin, J. K. Randolph, and K. C. Stanfield, Phys. Letters **29B**, 602 (1969).

³² G. McClellan, N. Mistry, P. Mostek, H. Ogren, A. Osborne, A. Silverman, J. Swartz, and R. Talman, and G. Diambri-Palazzi, Phys. Rev. Letters **23**, 718 (1969).

³³ G. Veneziano, Nuovo Cimento **57A**, 190 (1968).

³⁰ B. Y. Oh and W. D. Walker, Phys. Letters **28B**, 564 (1969).

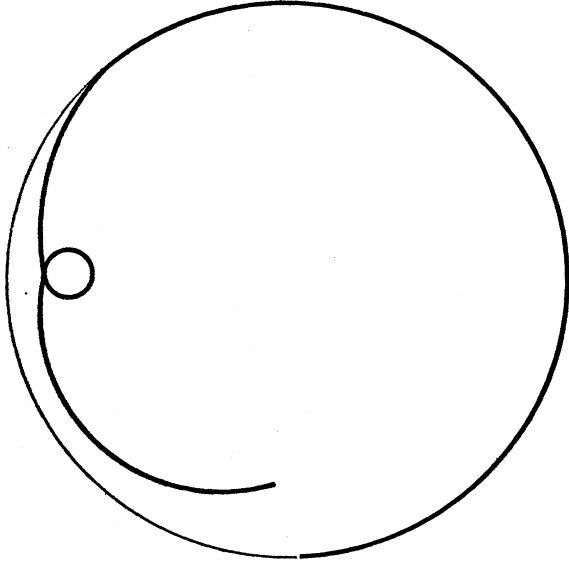


FIG. 16. Argand diagram illustration of a P -wave amplitude (ρ') which resonates. Note that for the P -wave amplitude shown, the ρ' signal would be about 1/10 of the ρ signal.

ACKNOWLEDGMENTS

We wish to thank many people for their cooperation. In particular, we thank the members of the 30-in. ANL-MURA chamber group, and especially Dr. L. Voyvodic for his cooperation. We thank our scanners and measurers for their help and cooperation. Our special thanks go to our supervisors, L. Boyd and S. Maggs. We thank our colleague Professor A. R. Erwin for his aid during the runs through the measurement period, and Professor L. Durand for many useful conversations in the course of the experiment.

APPENDIX A: OPE AMPLITUDES

The transition matrix element and cross section for the reaction $\pi(k_{\text{in}}) + N(P) \rightarrow \pi(k') + \pi(k'') + N(P')$ are defined by

$$\begin{aligned} \langle f | S-1 | i \rangle &= (2\pi)^4 i \delta^{(4)}(P_f - P_i) \langle f | T | i \rangle, \\ d\sigma &= \frac{(2\pi)^4}{F/2M} \left(\frac{1}{2} \sum_{\text{spins}} |\langle f | T | i \rangle|^2 \right) d\rho, \\ d\rho &= \frac{1}{(2\pi)^9} \frac{\pi dt}{F/2M} \left(\frac{k d\Omega_{\pi\pi} d m_{\pi\pi}^2}{4m_{\pi\pi}} \right)_{\pi\pi \text{ c.m.}} \quad (\text{A1}) \\ &= \frac{1}{(2\pi)^9} \frac{d^3 P'}{2P'^0/2M} \frac{d^3 k'}{2k'^0} \frac{d^3 k''}{2k''^0}, \end{aligned}$$

where the initial state will be specified by the proton helicity $|i\rangle = |\lambda\rangle$ and the final state by the helicities of the outgoing nucleon and dipion system $|f\rangle = |\mu\lambda'\rangle$.

$F=4Mk_{\text{lab}}$ is the flux factor, t is the squared four-momentum transfer to the nucleon; M and $m_{\pi\pi}=\sqrt{s}$ are masses of nucleon and dipion, respectively; and k and $\Omega_{\pi\pi}(\theta, \phi)$ refer to the momentum and scattering angles of the outgoing π^- in the $\pi\pi$ c.m. system. Out T is related to the nonrelativistic amplitude f by $T=8\pi(\sqrt{s_{\pi\pi}})f$ and $T=(8\pi(\sqrt{s_{\pi P}})/2M)f$ for the $\pi\pi$ and πp scattering, respectively.

The T matrix of the OPE process is (B for Born amplitude)

$$\begin{aligned} \langle \mu\lambda' | B | \lambda \rangle &= C_N g_{\pi NN} (u_\lambda \gamma_5 u_{\lambda'}) (t - m_\pi^2)^{-1} \\ &\quad \times \sum_l \sum_I d_{\mu 0^l}(-\psi) a_l^I Y_l^\mu(\theta, \phi) \quad (\text{A2}) \\ &= \sum_l \sum_I \langle \mu\lambda' | B_l^I | \lambda \rangle Y_l^\mu(\theta, \phi), \quad (\text{A3}) \end{aligned}$$

where $C_N=\sqrt{2}$ and 1 for the reactions (1) and (2), respectively, $g_{\pi NN}^2/4\pi=14.4\pm 0.4$; l and I refer to the partial wave and isospin of the $\pi\pi$ scattering. a_l^I is related to the $\pi\pi$ phase shifts and inelasticities (δ_l^I, η_l^I) by

$$\begin{aligned} a_l^I &= 8\pi m_{\pi\pi} C^I [\eta_l^I \exp(2i\delta_l^I) - 1/2ik] \\ &\quad \times [4\pi(2l+1)]^{1/2} G_l(t, s). \quad (\text{A4}) \end{aligned}$$

$G_l(t, s)$ is the off-shell correction factor to be discussed further below. The isospin factors of the $\pi\pi$ system C^I 's are explicitly

State	$I=0$	$I=1$	$I=2$
$\pi^-\pi^+$	$\frac{2}{3}$	1	$\frac{1}{3}$
$\pi^-\pi^0$	0	1	1
$\pi^0\pi^0$	$-\frac{1}{3}$	0	$\frac{2}{3}$
$\pi^-\pi^-$	0	0	1

(A5)

The Wigner d function appears in (A2) on account of the rotation required from the incoming pion direction in the $\pi\pi$ rest frame to the $\pi\pi$ helicity direction.¹¹ The angle ψ is related to the total c.m. scattering angle Θ and total c.m. momenta of the incoming and outgoing nucleons P, P' by (see Fig. 17)

$$\begin{aligned} k_{\text{off}} \sin\psi &= P \sin\Theta, \\ k_{\text{off}} \cos\psi &= P(\cos\Theta - \alpha')\gamma', \quad (\text{A6}) \end{aligned}$$

where

$$\begin{aligned} k_{\text{off}}^2 &= [t - (m_{\pi\pi} + m_\pi)^2][t - (m_{\pi\pi} - m_\pi)^2]/4s, \\ \alpha' &= [P'/(P'^2 + s)]^{1/2} [(P^2 + m_\pi^2)^{1/2}/P], \quad (\text{A7}) \\ \gamma' &= (P'^2 + s)^{1/2}/s^{1/2}. \end{aligned}$$

Explicit forms of the partial-wave amplitudes $\langle \mu\lambda' | B_l^I | \lambda \rangle$ of (A3), which are suitably absorption modified (A_l^I 's), are given in Appendix B. The angular distributions in θ and ϕ can be easily obtained from (A3). For this purpose, we introduce the density-

matrix elements

$$\rho_{\mu\mu'}^{ll'} = \frac{\sum_{\lambda\lambda'} (\sum_I \langle \mu\lambda' | A_I^I | \lambda \rangle) (\sum_I \langle \mu'\lambda' | A_I^{I'} | \lambda \rangle)^*}{\text{Tr} [\sum_{\lambda\lambda'} (\sum_I \langle \mu\lambda' | A_I^I | \lambda \rangle) (\sum_I \langle \mu'\lambda' | A_I^{I'} | \lambda \rangle)^*]} \quad (\text{A8})$$

and

$$Y_l^\mu = Y_l^\mu(\theta, \phi) \text{ with the } \exp(i\mu\phi) \text{ factor removed.} \quad (\text{A9})$$

With the dipion in a mixture of S , P , and D waves, we thus have

$$\begin{aligned} I(\cos\theta, \phi) = & \rho_{00}^{SS} (Y_0^0)^2 + \sum_{\mu} \rho_{\mu\mu}^{PP} (Y_1^\mu)^2 \\ & + \sum_{\mu} \rho_{\mu\mu}^{DD} (Y_2^\mu)^2 + 4\rho_{10}^{PP} Y_1^0 Y_1^0 \cos\phi \\ & + 2\rho_{1,-1}^{PP} Y_1^1 Y_1^{-1} \cos 2\phi + 4\rho_{21}^{DD} Y_2^1 Y_2^1 \cos\phi \\ & + 4\rho_{10}^{DD} Y_2^1 Y_2^0 \cos\phi + 4\rho_{20}^{DD} Y_2^2 Y_2^0 \cos 2\phi \\ & + 2\rho_{1,-1}^{DD} Y_2^1 Y_2^{-1} \cos 2\phi + 4\rho_{2,-1}^{DD} Y_2^2 Y_2^{-1} \cos 3\phi \\ & + 2\rho_{2,-2}^{DD} Y_2^2 Y_2^{-2} \cos 4\phi + 2\rho_{00}^{SP} Y_0^0 Y_1^0 \\ & + 4\rho_{01}^{SP} Y_0^0 Y_1^1 \cos\phi + 2\rho_{00}^{SD} Y_0^0 Y_2^0 + 4\rho_{01}^{SD} Y_0^0 Y_2^1 \cos\phi \\ & + 4\rho_{02}^{SD} Y_0^0 Y_2^2 \cos 2\phi + 2\rho_{00}^{PD} Y_1^0 Y_2^0 + 4\rho_{11}^{PD} Y_1^1 Y_2^1 \\ & + 4\rho_{01}^{PD} Y_1^0 Y_2^1 \cos\phi + 4\rho_{12}^{PD} Y_1^1 Y_2^2 \cos\phi \\ & + \rho_{10}^{PD} Y_1^1 Y_2^0 \cos\phi + 4\rho_{02}^{PD} Y_1^0 Y_2^2 \cos 2\phi \\ & + 2\rho_{1,-1}^{PD} Y_1^1 Y_2^{-1} \cos 2\phi + 4\rho_{1,-2}^{PD} Y_1^1 Y_2^{-2} \cos 3\phi. \quad (\text{A10}) \end{aligned}$$

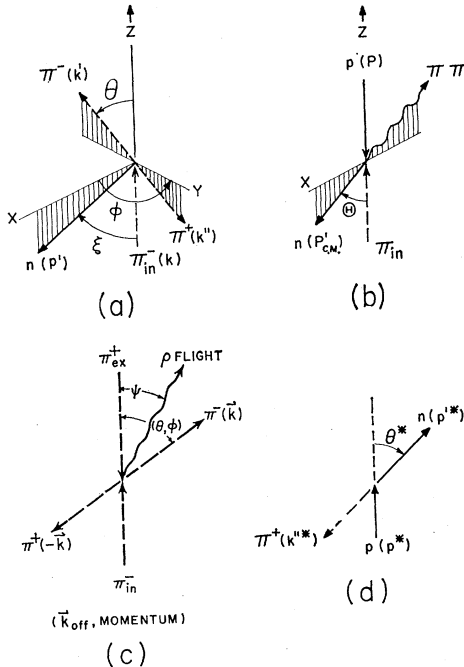


FIG. 17. Diagrams to illustrate kinematic relationships for the reaction $\pi^- p \rightarrow \pi^- \pi^+ n$. (a) In the $\pi^- \pi^+$ center-of-mass system; θ and ϕ are the usual $\pi\pi$ scattering angles. (b) In the over-all center-of-mass system; P and P' are the incoming and outgoing momenta of the nucleons (or π and $\pi\pi$). (c) In the $\pi^- \pi^+$ center-of-mass system; ρ flight direction is shown. (d) In the $\pi^+ n$ center-of-mass system. The nucleon scattering angle θ^* and momenta are indicated.

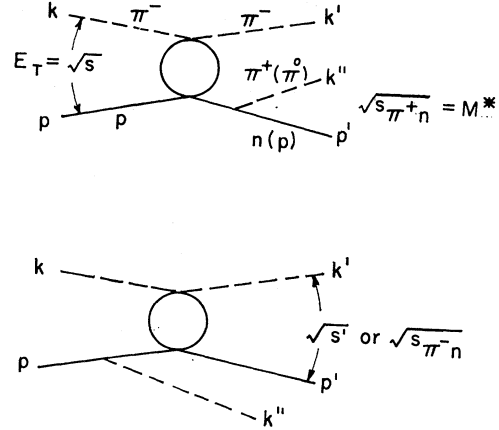


FIG. 18. Feynman diagrams of nucleon-pole terms of diffraction dissociation. Circles indicate pseudoelastic diffractive vertices. Notations of the kinematic quantities are defined.

Relatively simple cases of S and P waves, or D wave alone, are well known in the literature. Only the real parts of the density-matrix elements are implied in (A10). For the dipion in a mixture of S and P waves, we have

$$\begin{aligned} I(\cos\theta, \phi) = & (1/4\pi) \rho_{00}^{SS} + (\sqrt{3}/4\pi) \\ & \times (-2\sqrt{2} \text{Re} \rho_{01}^{SP} \sin\theta \cos\phi + 2\rho_{00}^{SP} \cos\theta) \\ & + (3/4\pi) (\rho_{00}^{PP} \cos^2\theta + \rho_{11}^{PP} \sin^2\theta - \sqrt{2} \text{Re} \rho_{10}^{PP} \\ & \times \sin 2\theta \cos\phi - \rho_{1,-1}^{PP} \sin^2\theta \cos 2\phi). \quad (\text{A11}) \end{aligned}$$

Finally for the $G_i(t, s)$ of (A4) we use the form suggested by Dürre and Pilkuhn,¹⁶ in analogy with the effect of penetration in potential scattering, namely,

$$G_i(t, s) = (k_{\text{off}}/k)^{\nu_i} \nu_i, \quad (\text{A12})$$

with

$$\begin{aligned} \nu_0 &= 1, \\ \nu_1 &= \left(\frac{1 + R^2 k^2}{1 + R^2 k_{\text{off}}^2} \right)^{1/2}, \\ \nu_2 &= \left(\frac{9 + 3R^2 k^2 + R^4 k^4}{9 + 3R^2 k_{\text{off}}^2 + R^4 k_{\text{off}}^4} \right)^{1/2}, \end{aligned}$$

where R is the radius of the $\pi\pi$ vertex, $R^2 \approx (10m_\pi^2)^{-1}$.

APPENDIX B: MODIFIED OPE AMPLITUDES

The absorption effects in the entrance and exit channels depend on the total angular momentum j and the helicities of the particles involved, among other things. We thus decompose (A2) or (A3) in the form

$$\langle \mu\lambda' | B | \lambda \rangle = \sum_j (j + \frac{1}{2}) \langle \mu\lambda' | B(j) | \lambda \rangle d_{\alpha\beta}^j(x),$$

$$x = \cos\theta, \quad \alpha = \lambda - \lambda', \quad \beta = 0 - \mu \quad (\text{B1})$$

and introduce the absorption with a replacement

$$\begin{aligned} \langle \mu\lambda' | B(j) | \lambda \rangle & \rightarrow (S_{\text{in}}^j)^{1/2} \langle \mu\lambda' | B(j) | \lambda \rangle (S_{\text{in}}^j)^{1/2} \\ & = \langle \mu\lambda' | A(j) | \lambda \rangle, \quad (\text{B2}) \end{aligned}$$

TABLE I. Normal form of $\langle \lambda' | A_S^{(t)} | \lambda \rangle$.

λ'	λ	$\langle \lambda' A_S^{(t)} \lambda \rangle = \frac{g_N g_{\pi NN}}{2PP'(z-x)} (1 - L_{ \lambda-\lambda' }) \times$
+	+	$\xi_- [\frac{1}{2}(1+x)]^{1/2} a_S^{(t)}$
+	-	$\xi_+ [\frac{1}{2}(1-x)]^{1/2} a_S^{(t)}$
-	+	$\xi_+ [\frac{1}{2}(1-x)]^{1/2} a_S^{(t)}$
-	-	$-\xi_- [\frac{1}{2}(1+x)]^{1/2} a_S^{(t)}$

where S_{fin} (S_{in}) is the S -matrix element in the exit (entrance) channel. We follow the formalism of Durand and Chiu¹² and write the modified amplitude as

$$\begin{aligned} \langle \mu \lambda' | A | \lambda \rangle &= \sum_j (j + \frac{1}{2}) \langle \mu \lambda' | A(j) | \lambda \rangle d_{\alpha\beta}^j(x) \\ &\times \exp[i(\alpha - \beta)\phi] \\ &= \langle \mu \lambda' | B | \lambda \rangle (1 - L_{|\alpha - \beta|}), \end{aligned} \quad (\text{B3})$$

where

$$\begin{aligned} L_\xi &= \int_0^\infty \exp[-y + g(y)] \left(1 + \frac{2y/\beta}{m_\pi^2 - t}\right)^{-\xi-1} dy, \\ g(y) &= \frac{2PP'(1-x)}{m_\pi^2 - t} \frac{2y^2/\beta}{m_\pi^2 - t + 2y/\beta}. \end{aligned} \quad (\text{B4})$$

β is a parameter which appears in the $d\sigma/dt$ of the $\pi\pi$ elastic scattering:

$$d\sigma/dt = (\sigma_T^2/16\pi) \exp(\beta t).$$

Following Durand and Chiu further, we remove the $j = \frac{1}{2}$ amplitude completely to obtain final forms of the modified OPE amplitudes. This is done by first writing (B3) in the form

$$\begin{aligned} \langle \mu \lambda' | A | \lambda \rangle &\sim [\frac{1}{2}(1-x)]^{1/2|\mu-\lambda'+\lambda|} [\frac{1}{2}(1+x)]^{1/2|\mu-\lambda'-\lambda|} \\ &\times [1/(z-x) + (\text{polynomials in } x)], \end{aligned} \quad (\text{B5})$$

TABLE II. Normal form of $\langle \mu \lambda' | A_P^{t=1} | \lambda \rangle$.

μ	λ'	λ	$\langle \mu \lambda' A_P^{t=1} \lambda \rangle = \frac{C_N g_{\pi NN}}{2PP'(z-x)} (1 - L_{ \lambda-\lambda'+\mu }) \times$
1	+	+	$\xi_- [\frac{1}{2}(1-x)]^{1/2} (1+z) (\epsilon_1/\sqrt{2}) a_p^{t=1}$
	+	-	$\xi_+ [\frac{1}{2}(1+x)]^{1/2} (1-z) (\epsilon_1/\sqrt{2}) a_p^1$
	-	+	$\xi_+ [\frac{1}{2}(1+x)]^{1/2} (1-x) (\epsilon_1/\sqrt{2}) a_p^1$
	-	-	$-\xi_- [\frac{1}{2}(1-x)]^{1/2} (1+x) (\epsilon_1/\sqrt{2}) a_p^1$
0	+	+	$\xi_- [\frac{1}{2}(1+x)]^{1/2} (z-\alpha) \epsilon_0 a_p^1$
	+	-	$\xi_+ [\frac{1}{2}(1-x)]^{1/2} (z-\alpha) \epsilon_0 a_p^1$
	-	+	$\xi_+ [\frac{1}{2}(1-x)]^{1/2} (z-\alpha) \epsilon_0 a_p^1$
	-	-	$-\xi_- [\frac{1}{2}(1+x)]^{1/2} (z-\alpha) \epsilon_0 a_p^1$
-1	+	+	$-\xi_- [\frac{1}{2}(1-x)]^{1/2} (1+x) (\epsilon_1/\sqrt{2}) a_p^1$
	+	-	$-\xi_+ [\frac{1}{2}(1+x)]^{1/2} (1-x) (\epsilon_1/\sqrt{2}) a_p^1$
	-	+	$-\xi_+ [\frac{1}{2}(1+x)]^{1/2} (1-z) (\epsilon_1/\sqrt{2}) a_p^1$
	-	-	$\xi_- [\frac{1}{2}(1-x)]^{1/2} (1+z) (\epsilon_1/\sqrt{2}) a_p^1$

where z is introduced through a relation

$$t - m_\pi^2 = -2PP'(z-x).$$

We then keep only the $1/(z-x)$ term (normal form) and discard the polynomial term, as the polynomial term affects only the lowest partial-wave amplitude of the πp and $(\pi\pi)N$ channels, which is to be suppressed by absorption.

The modified OPE amplitudes thus obtained are given in Tables I-III. We use the spinor normalization $\bar{u}u=1$ and

$$\gamma_5 = \begin{pmatrix} & 1 \\ 1 & \end{pmatrix}, \quad \gamma^0 = \begin{pmatrix} 1 & \\ & -1 \end{pmatrix}, \quad \boldsymbol{\gamma} = \begin{pmatrix} & -\boldsymbol{\sigma} \\ -\boldsymbol{\sigma} & \end{pmatrix}$$

TABLE III. Normal form of $\langle \mu \lambda' | A_D^{(t)} | \lambda \rangle$.

μ	λ'	λ	$\langle \mu \lambda' A_D^{(t)} \lambda \rangle = \frac{C_N g_{\pi NN}}{2PP'(z-x)} (1 - L_{ \lambda-\lambda'+\mu }) \times$	
2	+	+	$\xi_- [\frac{1}{2}(1+x)]^{1/2} (1-x) (1+z) (\frac{1}{4}\sqrt{6}) \epsilon_1^2$	
	+	-	$\xi_+ [\frac{1}{2}(1-x)]^{1/2} (1+x) (1-z) (\frac{1}{4}\sqrt{6}) \epsilon_1^2$	
	-	+	$\xi_+ [\frac{1}{2}(1-x)]^{1/2} (1-x^2) (\frac{1}{4}\sqrt{6}) \epsilon_1^2$	
1	-	-	$-\xi_- [\frac{1}{2}(1+x)]^{1/2} (1-x^2) (\frac{1}{4}\sqrt{6}) \epsilon_1^2$	
	+	+	$\xi_- [\frac{1}{2}(1-x)]^{1/2} (1+z) (z-\alpha) (\sqrt{\frac{3}{2}}) \epsilon_1 \epsilon_0$	
	+	-	$\xi_+ [\frac{1}{2}(1+x)]^{1/2} (1-z) (z-\alpha) (\sqrt{\frac{3}{2}}) \epsilon_1 \epsilon_0$	
	-	+	$\xi_+ [\frac{1}{2}(1+x)]^{1/2} (1-x) (z-\alpha) (\sqrt{\frac{3}{2}}) \epsilon_1 \epsilon_0$	
	-	-	$-\xi_- [\frac{1}{2}(1-x)]^{1/2} (1+x) (z-\alpha) (\sqrt{\frac{3}{2}}) \epsilon_1 \epsilon_0$	
	0	+	+	$\xi_- [\frac{1}{2}(1+x)]^{1/2} [3\epsilon_0^2 (z-\alpha)^2 - 1]$
+		-	$\xi_+ [\frac{1}{2}(1-x)]^{1/2} [3\epsilon_0^2 (z-\alpha)^2 - 1]$	
-		+	$\xi_+ [\frac{1}{2}(1-x)]^{1/2} [3\epsilon_0^2 (z-\alpha)^2 - 1]$	
-		-	$-\xi_- [\frac{1}{2}(1+x)]^{1/2} [3\epsilon_0^2 (z-\alpha)^2 - 1]$	
-1		+	+	$-\xi_- [\frac{1}{2}(1-x)]^{1/2} (1+x) (z-\alpha) (\sqrt{\frac{3}{2}}) \epsilon_1 \epsilon_0$
		+	-	$-\xi_+ [\frac{1}{2}(1+x)]^{1/2} (1-x) (z-\alpha) (\sqrt{\frac{3}{2}}) \epsilon_1 \epsilon_0$
	-	+	$-\xi_+ [\frac{1}{2}(1+x)]^{1/2} (1-z) (z-\alpha) (\sqrt{\frac{3}{2}}) \epsilon_1 \epsilon_0$	
	-	-	$\xi_- [\frac{1}{2}(1-x)]^{1/2} (1+z) (z-\alpha) (\sqrt{\frac{3}{2}}) \epsilon_1 \epsilon_0$	
	-2	+	+	$\xi_- [\frac{1}{2}(1+x)]^{1/2} (1-x^2) (\frac{1}{4}\sqrt{6}) \epsilon_1^2$
		+	-	$\xi_+ [\frac{1}{2}(1-x)]^{1/2} (1-x^2) (\frac{1}{4}\sqrt{6}) \epsilon_1^2$
-		+	$\xi_+ [\frac{1}{2}(1-x)]^{1/2} (1+x) (1-z) (\frac{1}{4}\sqrt{6}) \epsilon_1^2$	
-		-	$-\xi_- [\frac{1}{2}(1+x)]^{1/2} (1-x) (1+z) (\frac{1}{4}\sqrt{6}) \epsilon_1^2$	

and introduce the notations

$$\xi_{\pm} = \left(\frac{E'+M}{2M} \frac{E+M}{2M} \right)^{1/2} \left(\frac{P}{E+M} \pm \frac{P'}{E'+M} \right),$$

where E and P (E' and P') are the energy and momentum of the incoming (outgoing) nucleon in the total c.m. system. Other symbols used are

$$\epsilon_0 = \gamma' P'/k_{\text{off}}, \quad \epsilon_1 = P'/k_{\text{off}}.$$

APPENDIX C: NUCLEON-POLE TERMS

Nucleon-pole terms of the diffraction dissociation,¹⁴ shown in Fig. 18, are summarized here. We assume in our calculation (i) that the πN diffraction vertex, indicated by a circular blob, is identical to that of high-energy forward elastic scattering with a T matrix given

by

$$T_{\pi N} = i \frac{2(s_{\pi N})^{1/2} k_{\pi N \text{ c.m.}}}{2M} \sigma_T(s_{\pi N}) \exp(\frac{1}{2}\beta t_{\pi\pi}), \quad (\text{C1})$$

with $\beta \approx 9$ (GeV/c) $^{-2}$ for 7-GeV/c π^-p . Here $k_{\pi N \text{ c.m.}}$ is the momentum of the π in the πN rest frame, and $\sigma_T(s_{\pi N})$ is that of the total πN cross section. We assume, furthermore, (ii) that the π -emission vertex is due to a P -wave $\pi N \bar{N}$ coupling, which gives $C_N g_{\pi N \bar{N}} \bar{u}_\lambda \gamma_5 u_\lambda$ for the vertex part.

For the T matrix of the nucleon-pole terms, we obtain [see Fig. 18 for notations; we take reaction (1) for definiteness]

$$\begin{aligned} \langle \lambda' | T_{\text{NPT}} | \lambda \rangle = & \frac{\sqrt{2} g \bar{u}_\lambda \gamma_5 (\mathbf{p}' + \mathbf{k}' + M) u_\lambda}{s_{\pi^+ n} - M^2} T_{\pi^- p} \\ & + \frac{\sqrt{2} g \bar{u}_\lambda (\mathbf{p}' - \mathbf{k}' + M) \gamma_5 u_\lambda}{-(s_{\pi^+ n} - M^2 - m_\pi^2 + t - t_{\pi\pi})} T_{\pi^- n}. \quad (\text{C2}) \end{aligned}$$

$T_{\pi^- p}$ and $T_{\pi^- n}$ refer to the πN diffraction vertices, of the form (C1), and the denominator of the second term is given in a convenient form. (C2) can be simplified in the form

$$\begin{aligned} \langle \lambda' | T_{\text{NPT}} | \lambda \rangle = & \sqrt{2} g (\bar{u}_\lambda \gamma_5 \mathbf{k}' u_\lambda) \\ & \times \left(\frac{T_{\pi^- p}}{s_{\pi^+ n} - M^2} - \frac{T_{\pi^- n}}{s_{\pi^+ n} - M^2 - m_\pi^2 + t - t_{\pi\pi}} \right). \quad (\text{C3}) \end{aligned}$$

In a realistic treatment of the nucleon-pole terms, we need to make an appropriate correction for the absorption in the entrance and exit channels. As the T matrix of the diffraction vertex (C1) already includes absorption effects in one channel, we need to modify (C3) by a multiplication with a factor $(1 - L_{|\lambda-\lambda'|})^{1/2}$ when the kinematic configuration for (C3) is identical to the appropriate kinematic configuration for the factor $(1 - L_\xi)$ of Eq. (B3). Thus we have

$$\langle \lambda' | T_{\text{NPT}} | \lambda \rangle = [\text{expression in (C3)}] \times (1 - L_{|\lambda-\lambda'|})^{1/2}. \quad (\text{C4})$$

The invariant amplitudes (C4) can be easily evaluated in terms of the variables in the $\pi^+ n$ c.m. system. In practice, we need to express (C4) in terms of variables which are natural for the OPE process, namely, t , $m_{\pi\pi}$, $\cos\theta$, and ϕ ("OPE variables"). We carry out this program in the remainder of this appendix. Denoting the energy momenta of the particles (see Fig. 18) in the $\pi^+ n$ c.m. system by asterisks, and denoting the $p \rightarrow n$ scattering angle in the $\pi^+ n$ c.m. system by θ^* [see

Fig. 17(d)], we have

$$\begin{aligned} \bar{u}_+ \gamma_5 \mathbf{k}'' u_+ &= (-\xi_+^* k_0''^* - \eta_+^* P'^*) \cos \frac{1}{2} \theta^*, \\ \bar{u}_- \gamma_5 \mathbf{k}'' u_+ &= (\xi_-^* k_0''^* - \eta_-^* P'^*) \sin \frac{1}{2} \theta^*, \\ \bar{u}_+ \gamma_5 \mathbf{k}'' u_- &= (\xi_-^* k_0''^* - \eta_-^* P'^*) \sin \frac{1}{2} \theta^*, \\ \bar{u}_- \gamma_5 \mathbf{k}'' u_- &= (\xi_+^* k_0''^* - \eta_+^* P'^*) \cos \frac{1}{2} \theta^*, \end{aligned} \quad (\text{C5})$$

where

$$\begin{aligned} \xi_{\pm}^* &= \left(\frac{E'^* + M}{2M} \right)^{1/2} \left(\frac{E^* + M}{2M} \right)^{1/2} \left(\frac{P^*}{E'^* + M} \pm \frac{P'^*}{E^* + M} \right), \\ \eta_{\pm}^* &= \left(\frac{E'^* + m}{2M} \right)^{1/2} \left(\frac{E^* + M}{2M} \right)^{1/2} \left(1 \pm \frac{P'^*}{E'^* + M} \frac{P^*}{E^* + M} \right). \end{aligned} \quad (\text{C6})$$

Thus (C4) can be written in terms of "OPE variables" and $s_{\pi^+ n}$ by noting that

$$\begin{aligned} (P^*)^2 &= [t_{\pi\pi} - (m_{\pi^+ n} + M)^2][t_{\pi\pi} - (m_{\pi^+ n} - M)^2]/4s_{\pi^+ n}, \\ (P'^*)^2 &= [s_{\pi^+ n} - (M + m_\pi)^2][s_{\pi^+ n} - (M - m_\pi)^2]/4s_{\pi^+ n}, \end{aligned} \quad (\text{C7})$$

and

$$\begin{aligned} -t &= -2M^2 + 2(P^{*2} + M^2)^{1/2}(P'^{*2} + M^2)^{1/2} \\ &\quad - 2P^* P'^* \cos \theta^*. \end{aligned}$$

The only remaining problem now is to write $s_{\pi^+ n}$ in terms of "OPE variables." Referring to Fig. 17(a), which shows the kinematics of the reaction $\pi^- p \rightarrow \pi^- \pi^+ n$ in the $\pi\pi$ rest frame, we have

$$\begin{aligned} s_{\pi^+ n} &= (k_\mu'' + P_\mu')^2 \\ &= m_\pi^2 + M^2 + (2E'\omega'' - 2\mathbf{P}' \cdot \mathbf{k}'')_{\pi\pi \text{ c.m.}}, \end{aligned} \quad (\text{C8})$$

where (ω'', \mathbf{k}'') and (E', \mathbf{P}') denote the energy-momenta of π^+ and n , respectively. We introduce the angle ξ [Fig. 17(a)] related to the c.m. scattering angle θ by

$$(P' \sin \xi)_{\pi\pi \text{ c.m.}} = (P' \sin \theta)_{\text{tot c.m.}}$$

Also,

$$(2E'\omega'')_{\pi\pi \text{ c.m.}} = (s_{\text{tot}} - M^2 - s_{\pi\pi}). \quad (\text{C9})$$

The $(-2\mathbf{P}' \cdot \mathbf{k}'')$ $_{\pi\pi \text{ c.m.}}$ term in (C8) can be written with the help of the angles θ , ϕ , and θ to give

$$\begin{aligned} s_{\pi^+ n} &= m_\pi^2 + M^2 + (2E'\omega'')_{\pi\pi \text{ c.m.}} - 2(|\mathbf{P}'| |\mathbf{k}''|)_{\pi\pi \text{ c.m.}} \\ &\quad \times (\sin \xi \sin \theta \cos \phi + \cos \xi \cos \theta). \end{aligned} \quad (\text{C10})$$